Engineering Structures 291 (2023) 116465

Contents lists available at ScienceDirect

Engineering Structures

journal homepage: www.elsevier.com/locate/engstruct

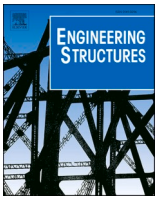

Preliminary structural and seismic performance assessment of the Mosque-Cathedral of Cordoba: The Abd al-Rahman I sector

M.V. Requena-Garcia-Cruz [a,*], E. Romero-Sánchez [b], M.P. López-Piña [b], A. Morales-Esteban [b,c]

[a] Department of Mechanical Engineering and Industrial Design, University of Cadiz, Spain
[b] Department of Building Structures and Geotechnical Engineering, University of Seville, Spain
[c] Instituto Universitario de Ciencias de la Construcción, University of Seville, Spain

ARTICLE INFO

Keywords:
Structural and seismic performance
Finite element method
Nonlinear analyses
UNESCO World Heritage Site
Numerical modelling
Masonry buildings

ABSTRACT

This manuscript discusses some preliminary results on the structural and the seismic performance of the Mosque-Cathedral of Cordoba, a UNESCO World Heritage. The area is characterized by a moderate seismic hazard. The building was built from the 8th to the 16th century and it has undergone several transformations. Owing to the complexity of the building, this work has focused on the assessment of the Abd al-Rahman I sector, which is the most aged part of the complex. For that, first, a 3D numerical finite element model of the sector has been done in the OpenSees framework and calibrated. To do so, an experimental non-destructive campaign has been carried out. Second, the model has been used to evaluate the structural behaviour, under vertical and horizontal loads, considering different scenarios. Finally, the crack patterns and the seismic safety have been obtained. The results showed that the numerical damage obtained for the gravitational loads is in good agreement with the data collected from the in situ surveys. Also, particular attention should be paid to the cymatiums, as they are the most demanded part of the system. Regarding its seismic performance, the building presents a higher capacity in the direction of the arcades. For the seismic demand, slight damage is expected in both principal directions of the building, which could be easily repaired. Damage concentration is expected in the contact between the perimetral wall and the arcades. This work has expanded the study of the features of the Mosque-Cathedral of Cordoba to the structural and seismic analysis with advanced numerical FE computing, which has not been done to date. To the authors' knowledge, this is the first time that a macro-modelling approach with solid elements is presented for the seismic assessment of heritage buildings using the OpenSees framework. The methodology to do so is also presented. Apart from showing how advanced numerical analyses can provide useful information to assess the existing damage on monumental buildings, this work aims at contributing to the assessment of the vulnerability and the safety of one of the most emblematic mosque-like buildings of the world.

1. Introduction

1.1. Importance of the structural assessment of heritage buildings

Built cultural heritage embodies the identity of cultures and regions. It provides information on the technical and the cultural achievements of a specific period or population [1]. These features characterise the Great Mosque-Cathedral of Cordoba, located in the region of Andalusia, in southern Spain. The complex was declared by the UNESCO as a World Heritage Site in 1984 [2]. This protection was extended to its surroundings, the Historic Centre of Cordoba, in 1994. In 2014, the UNESCO awarded the complex with the recognition of 'Site of Outstanding Universal Value'.

The Mosque-Cathedral of Cordoba is one of the most important monuments in Spain. Its construction started in the 8th century and it was completed in the 16th, undergoing several extensions and transformations. The building is characterized by the wideness of its space, its size and its building techniques. It is composed of parallel naves made of masonry walls and arches with shafts and capitals of stone, following a mosque-like configuration. Owing to its features, it has greatly influenced Western and Eastern Islamic and Christian architectures [2]. Therefore, the preservation of such a monumental asset is crucial.

In the case of the Mosque-Cathedral of Cordoba, several features have been studied, such as its proportions and distribution [3,4], columns organisation system [5] or its acoustic properties [6]. As pointed

* Corresponding author at: Department of Mechanical Engineering and Industrial Design, University of Cadiz, Spain (M.V. Requena-Garcia-Cruz).
E-mail addresses: mariavictoria.requena@uca.es (M.V. Requena-Garcia-Cruz), eromero13@us.es (E. Romero-Sánchez), mlopez24@us.es (M.P. López-Piña), ame@us.es (A. Morales-Esteban).

https://doi.org/10.1016/j.engstruct.2023.116465
Received 10 January 2023; Received in revised form 3 May 2023; Accepted 9 June 2023
Available online 16 June 2023

Nomenclature

Mechanical parameters of materials

f_c	Compressive strength. Subindexes '0', 'p' and 'r' refer to elastic, peak and residual strength
f_{Mc}	Compressive strength of masonry
$f_{M,k}$	Characteristic compressive strength of masonry
f_{bc}	Compressive strength of brick or stone
f_{mc}	Compressive strength of mortar
f_t	Tensile strength
f_{Mt}	Tensile strength of masonry
ε_c	Compressive strain. Subindex 'p' refers to peak strength
ε_t	Tensile strain

Analyses and parameters computed

EF	Equivalent frame
FE	Finite element
NDT	Non-destructive test
NLSA	Nonlinear static analysis
OMA	Operational modal analysis
PBA	Performance-based approach
G_{fc}	Compressive fracture energy
G_{ft}	Tensile fracture energy
l_{ch}	Element characteristic length
E	Young's modulus
ν	Poisson ratio
G	Shear modulus
ρ	Density
σ	Standard deviation
PL	Performance level
DL	Damage level
V_b	Basal shear force
W	Weight of the system
d_{top}	Displacement of the control node on the top
d_{tb}	Seismic demand displacement

out in [5], owing to the complexity of the asset, most of these previous studies focused on sectors into which the building is divided. Although many researchers have evaluated this complex building, none of them has studied in depth its structural features.

Structural analysis plays a key role in the diagnosis and the safety assessment of historic buildings [7]. It enables characterising their current state, better understanding their structural features and determining their level of structural safety. Furthermore, structural analysis is essential in monumental buildings built following old techniques in seismic areas such as Cordoba. This region has a moderate seismic activity, due to the convergence between the Eurasian and the African tectonic plates [8]. It is distinguished by intraplate close earthquakes of moderate magnitude and far away earthquakes of large/very large magnitude with long return periods [9,10].

Studies focused on the conservation and the restoration of historic buildings are complex from the structural and seismic analysis point of view [11]. This is mainly due to [12]: i) their aseismic design; ii) the transformations undergone; and iii) the difficulty of acquiring *as built* information of the structural elements and the materials. Nevertheless, improving assessment methodologies and the level of knowledge of cultural assets is key to guarantee their conservation and to carry out future interventions [13,14]. On this basis, the careful analysis of case studies or sectors provides helpful information that can be analogically applied for its rehabilitation and reconstruction [15].

1.2. Modelling strategies for heritage buildings

There are several methods and modelling strategies to assess the structural and the seismic behaviour of masonry heritage buildings. In [16], a critical review of the different strategies, ranging from the Equivalent Frame EF) method (commonly used in engineering practice) to more refined techniques like 2D and 3D Finite Element (FE) procedures based on continuous, discrete, and micro-mechanical approaches is presented. Above all, the FE method is the most powerful and frequently used modelling approach for the structural and the seismic response of heritage buildings. The EF has been used to model mosque-like buildings in 3D [17,18]. However, it leads to certain simplifications, such as the impossibility to obtain the concentrated damage for small deformations, among others, that the FE method does not present [19,20].

Focusing on the FE method, two distinct modelling approaches can be found as presented in [21]: the continuous or the discrete approaches. The continuous approach discretizes the masonry's walls using beam, shell and solids elements. The discrete approach, considers the masonry as an assembly of blocks that can impact and slide between them. The continuous or macro modelling technique uses a homogeneous and isotropic material to simulate the behaviour of the structural elements. It is usually a damage-plasticity model that allows representing the different masonry capacities in tension and compression through different constitutive laws. Contrariwise to the discrete approach, a homogenization between the bricks and mortar characteristics is considered [22]. Despite its limitation compare to the discrete approach, the continuous method has been proved sufficiently efficient and a robust method to obtain the response of different typologies of historical constructions, as discussed in [23]. Furthermore, this is the approach that is commonly used to model singular heritage buildings such as domes [24–26], towers [27,28], palaces [20], churches [21,29] or mosques [18,30].

In order to provide a reliable safety assessment, it is necessary to obtain numerical models validated and calibrated [31]. This is usually done through an in situ investigation plan based on non-destructive tests (NDT). NDT enable surpassing the difficulty/impossibility of carrying out destructive tests on historic buildings. These allow gathering information about the most relevant parameters, such as the mechanical properties of the materials and the stiffness of the system. The operational modal analysis (OMA) is one of the most used NDT to calibrate numerical models, particularly for complex ancient buildings [7,32–34].

1.3. Performance assessment of heritage buildings

The behaviour of heritage buildings can be either obtained through nonlinear static analyses (NLSA) and/or dynamic analyses, such as time-history or incremental. The type of analysis is a very critical point since the type of result obtained has a direct consequence in the decision-making of both the assessment and latter retrofitting of the asset [35]. Dynamic analyses are a more accurate method to simulate the behaviour of buildings, especially heritage ones. In dynamic analyses, the contribution of all modes is considered. Also, the effect of the vertical component of the input motions is contemplated which, in special structures like heritage buildings, cannot be omitted. Furthermore, this method does not need to perform the conventional transformation to an equivalent nonlinear single degree of freedom system, since the seismic demand is directly described in terms of acceleration time history, obtaining more accurate results. Contrariwise, NLSA does not consider the seismic input, as the displacement demand is evaluated later by applying capacity-demand methods, like the N2-method. Despite such pros, dynamic analyses are more time consuming and require a high computational burden.

In spite of some inherent limitations of NLSA, as mentioned above,

NLSA represents an effective and feasible tool for the analysis of heritage structures. In fact, NLSA is nowadays extensively used not only at research level but also in the engineering practice. Compared to dynamic analyses, NLSA allows an easier formulation of the monotonic behaviour of URM panels (it does not require to simulate their cyclic behaviour and a lower computational burden is required). The performance of NLSA requires proper choices concerning: the seismic load pattern, the selection of the control node and the representative displacement to be considered in the pushover curve. All of them affect the pushover curve obtained and they are particular important in irregular buildings without rigid diaphragms. In [27], the results obtained with both types of analysis exhibited a satisfactory match, suggesting similar conclusions for the seismic vulnerability of the heritage buildings analysed. Furthermore, as concluded in [36], NLSA can be used as a first attempt to assess the seismic behaviour of complex heritage buildings, bearing in mind that more complex dynamic analyses are needed to compare the results. Further information on the pros and cons of each type of analyses on heritage structures, particularly URM ones, was presented in [37].

For the evaluation of the seismic safety of heritage buildings, the performance-based approach (PBA) is commonly adopted. This is grounded on the fulfilment of some target performance levels in correspondence to predefined seismic actions [12]. The performance of the buildings can be obtained via NLSA and the verification of the capacity-demand method (among other methos as listed in [12]). NLSA and the PBA have been effectively used to assess the structural and the seismic performance of heritage buildings like minarets [38], old mosques [17,18] and churches [39].

1.4. Scope of this work

This work aims to assess, as a preliminary study, the structural and the seismic performance of the Great Mosque-Cathedral of Cordoba. Given the recent historiography of the Mosque-Cathedral of Cordoba pointed out in the state of the art, this work expands the study of its features to the structural and the seismic analysis. This work has not been done yet on this building, despite its cultural value and the seismic hazard of the area. Owing to the complexity of the building, as a preliminary study, this work has focused on the assessment of the Abd al-Rahman I sector in detail. This is the oldest part of the building, which was finished in the 8th century.

Apart from studying the structural features of this building for the first time with advanced methods, the main novelty of this work is the methodology presented to achieve the goal established. The analyses have been carried out in the OpenSees framework. This is an open-source software, specific for earthquake-engineering issues. This type of buildings has not been developed in depth in this framework. Hence, as a novelty, an integrated methodology for a mosque-like building is presented, specifically developed to be used in the OpenSees framework. The methodology combines FE analysis, macro-mechanical modelling and experimental NDT for the validation of analytical analyses. Given the state-of-the-art analysis, above all, the FE method is the most powerful and frequently used modelling approach for the structural and seismic assessment. For this reason, the results obtained in this paper can be used in future research works but also for practitioners, especially for the maintenance and the retrofitting plans of the complex.

Furthermore, the results obtained have allowed to assess and to discuss both the building's internal damage and its cracking pattern. The numerical model has been subsequently employed to provide a first evaluation of the seismic behaviour of the building. Apart from showing how advanced numerical analyses can provide useful information to assess the existing damage of monumental buildings, this work aims at contributing to the assessment of the vulnerability and the safety of one of the most emblematic mosque-like buildings of the world.

On this basis, this document is divided as follows. In §2, a summary on the history, the features and the historic transformations of the Mosque-Cathedral of Cordoba has been presented. In §3, a preliminary assessment of the current state of the Abd 'al-Rahman I sector has been performed. Knowledge of the structure evolving in the in situ NDT experimental campaign (according to the state of the art review), the material parameters and the structural identification has been provided. In §4, the PBA has been presented together with the selected Performance Levels (PL) and the seismic input. In §5, the nonlinear FE numerical modelling has been developed, validated and calibrated through the experimental results derived from the NDTs and the available data. In this work, the FE method has been chosen since it is the most powerful modelling method. It has been combined with the macro-mechanical modelling approach. It allows obtaining robust results for a preliminary and a global analysis with a fair computational burden and time. In §6, the NLSA have been carried out under vertical and horizontal loads considering different scenarios. Since, in this research, it is intended to develop a calibrated and validated model, NLSA have been chosen, bearing in mind the limitations and the simplifications of this type of analysis. These limitations and implications are intrinsic to the method. Hence, to obtain reliable results, proper choices concerning the load pattern, the control node and the representative displacement have been considered. As pointed out, all of them affect the pushover curve and are particular important. A study concerning the effects of different horizontal load patterns and different control nodes on the structural response has been shown. Simultaneously, the crack patterns obtained from the numerical analysis have been discussed. Afterwards, the seismic safety assessment has been presented. In §7, the conclusions and the future developments have been presented. A flowchart to summarize the methodology path followed in this work is presented in Fig. 1.

2. The Great Mosque-Cathedral of Cordoba

2.1. General information and extensions

Located in southern Spain, the Great Mosque-Cathedral of Cordoba constitutes one of the most representative buildings of Andalusian architecture and of emblematic Hispano-Muslim Umayyad art [2]. It is a diaphanous structure that has gone through various extensions, finally reaching an overall dimension of 130 m in length and 50 m in width. The building was constructed for a religious purpose and it has three differentiated elements (Fig. 2(a)): the minaret, a rectangular hypostyle hall or *liuán* conceived as a prayer room with naves perpendicular to the *qibla* (where the *mihrab* is placed) and a proportionally harmonic patio or *sahn*. In the design of the Great Mosque-Cathedral of Cordoba, elements hitherto unheard-of in Islamic religious architecture were used [2]. Such is the case of the double arches (the lower one in the form of a horseshoe and the upper one semi-circular) to create the parallel naves (Fig. 2(b)) or the 'honeycomb' capital (Fig. 2(c)), which differs from the Corinthian capital, typical of the caliph art [40].

The Great Mosque-Cathedral of Cordoba has been in constant evolution, subjected to reforms and extensions to be adapted to the needs of the period, like transitioning from Islamic to Christian worship [40]. The construction of the Abd al-Rahman I mosque was started in 785 and it was formed by eleven naves to house eleven thousand worshippers. The original mosque was enlarged three different times following the original design [6] (Fig. 3): by Abd al-Rahman II in 852, Al Hakam in 970 and Al Mansour in 988 [41]. In the 13th century, Cordoba's Great Mosque was transformed into a cathedral, which also involved the construction of different defensive structures in the Historic Centre. In the 16th century, the Renaissance cruciform basilica was built in a Plateresque style [40]. Over the years, different chapels and domes were added within the reticula of columns and arcades. The building, with its juxtaposition of cultures and architectural styles, has grown organically and continuously over two millennia, maintaining its material integrity, as the UNESCO report stated [2].

The first mosque adopted the orientation of a previous Christian church, which was convenient due to its orientation towards the

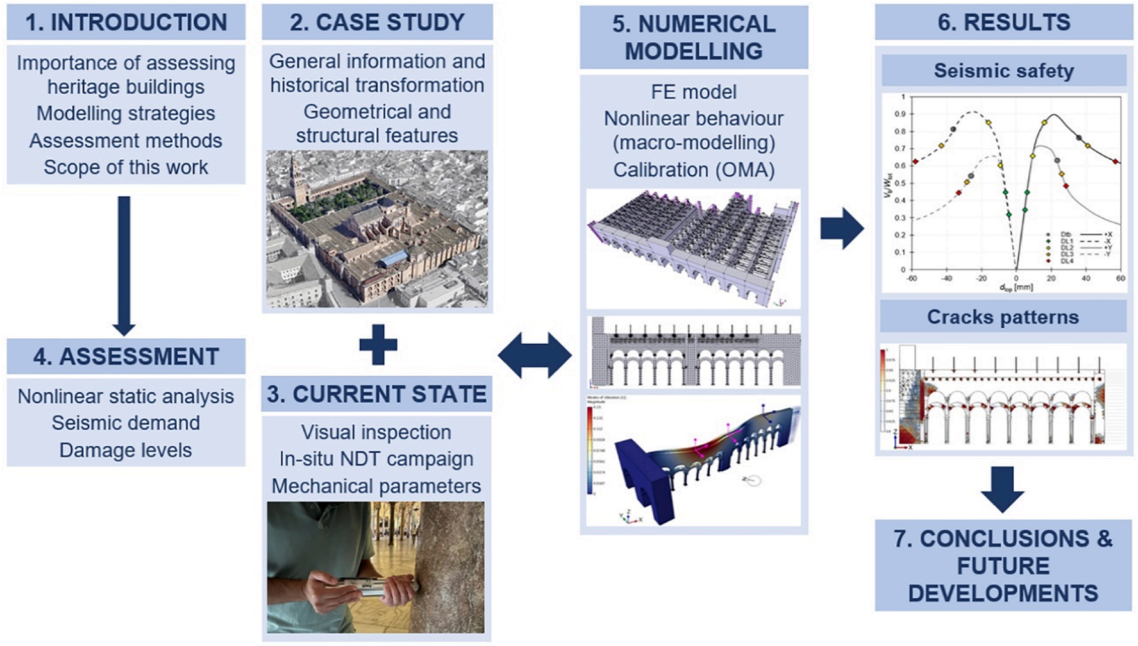

Fig. 1. Methodology followed in this study.

(a) (b) (c)

Fig. 2. (a) General view of the complex and the Guadalquivir River. Internal photographs, taken by the authors, of the Mosque with particular emphasis on the naves configuration and the coffered ceiling (b), and the double arches (c).

Guadalquivir River [41] (Fig. 2(a)). The successive extensions followed the same scheme, resulting in a South-West oriented mosque (Fig. 4(a)). The construction of the primitive part of the mosque (the Abd al-Rahman I, the Abd al-Rahman II and the Al Hakam sectors) was made by reusing existing materials (or plunder). Their bases, shafts and capitals come from existing and dismantled buildings (Roman, Catholic and Arabic) in the region. Consequently, materials vary from marble, granite to limestone. The double arches were made with stone voussoirs and bricks, creating its characteristic bichromatism (Fig. 4(b)). By contrast, the Al Mansour sector was constructed using mainly new materials. It followed a slightly different and more sophisticated building methodology, based on Byzantine architecture [40]. In this sector, the voussoirs were built entirely with stone. The levels of the different elements vary to achieve a global homogenous horizontal line on top of the capitals.

2.2. The Abd 'al-Rahman I sector

The Abd 'al-Rahman I sector is composed of eleven longitudinal naves, with different widths ranging from 6.83 m to 7.83 m. In total, the sector is 90 m wide and 20 m long. In Fig. 5, a plan of the sector analysed is shown, pointing out the interaction/contact with other sectors. There are stone columns formed by bases, shafts, capitals and cymatiums that date from the Roman and the Visigothic period [5] (Fig. 6). On the top of the arches, the 'aqueducts' evacuate the rainwater and support the timber roofing (Fig. 7(a)). These walls are made of brick limestone masonry. Below, there is a coffered ceiling composed of timber beams of 80–90 cm span, which are lightly embedded on top of the walls. Most of the timber roofing of the naves was changed for steel trusses in the early 20th century (Fig. 7(b)). In this sector, only N14 still has the timber roofing. The rest of the naves N9-N13 and N15-N19 have the 20th century steel trusses. The walls on the perimeter are composed of limestone masonry. Some openings of the north wall were filled.

3. Preliminary assessment of the current state

The Great Mosque-Cathedral of Cordoba is characterised by its complexity and size. Depending on the date of construction, each sector presents different configurations and materials. Therefore, they are

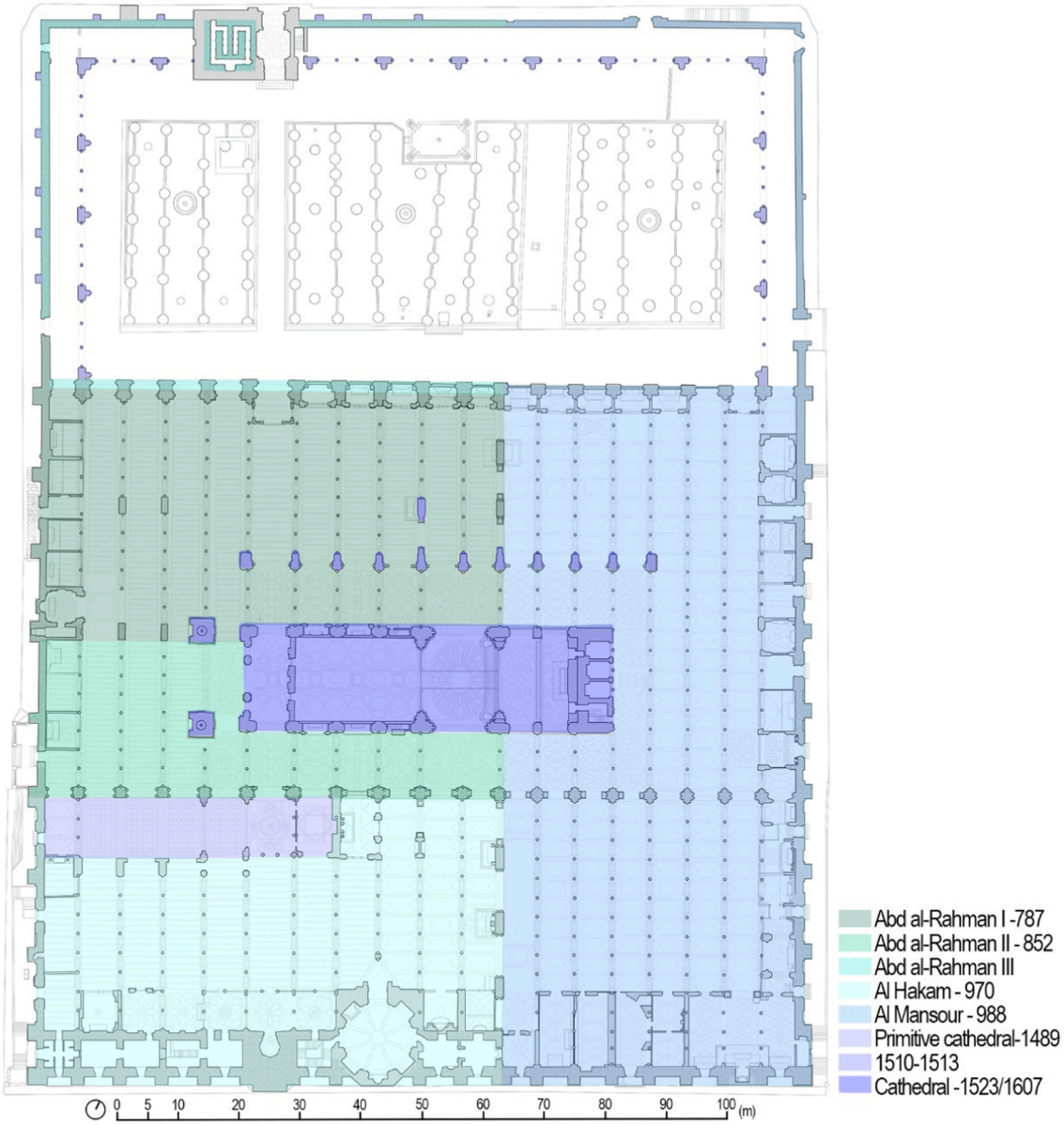

Fig. 3. Plan view with the indication of the extensions in the building adapted from [41]

expected to perform differently structurally and in the case of an earthquake. Given this, the careful analysis of the different sectors and elements that compose the asset is essential for its overall understanding. Accordingly, as suggested by [12], reliable models are needed for historic buildings to guarantee their conservation and to avoid exceeding calculations. On that premise, a detailed structural and seismic performance assessment is carried out on the Abd 'al-Rahman I sector. To do so, a thorough analysis of its structural features and particularities for a robust modelling and calibration has been performed. This is the primitive area, which, therefore, contains most of the reused material. Furthermore, this sector has been chosen to be analysed as a first step for the study of the entire complex.

In this section, the procedure followed for the assessment of the current state of the Abd 'al-Rahman I sector is presented. A comprehensive inspection and diagnosis campaign has been performed to distinguish its main structural aspects. The activities carried out on site included the structural identification and characterisation, the visual inspection and the NDT. For the analyses and the construction of the 3D model, the historic drawings (plans and cross sections) belonging to the studies of [41] were used as the main reference. In §3.1, the results of the visual inspection are presented. In §3.2, the in situ testing campaign is described along with the analysis of the mechanical properties of the materials.

3.1. Visual inspection

According to the literature and the information provided by the maintenance group of the building, there is no apparent damage in any of the sectors of the building. The building has an exhaustive monitoring and conservation plan. Hence, it is in constant refurbishment. If there had been damage, it was automatically repaired. Hence, it is not possible to analyse visually the damage that the building has had. The identification of the material of the columns has been performed by means of a visual inspection and this has been corroborated with the work developed in [5].

3.2. In situ testing and available data revision

3.2.1. Schmidt Hammer tests

The Schmidt Hammer Method test has been carried out to extract

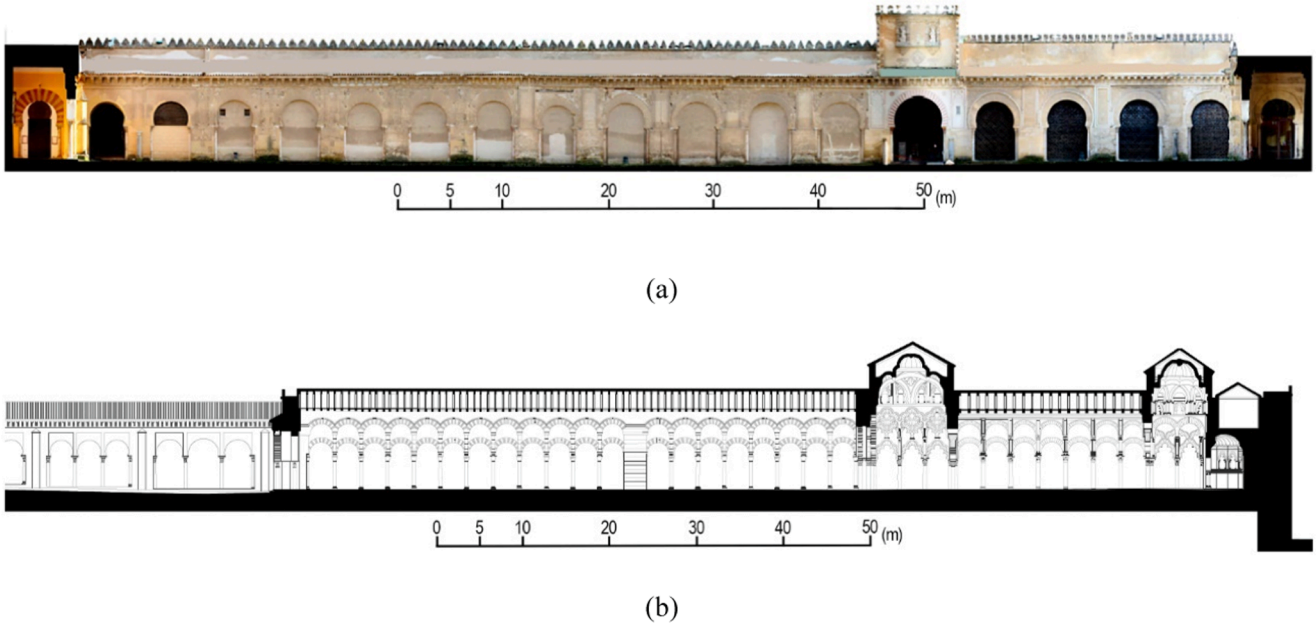

Fig. 4. Façade to the patio (a) and north–south section of the Abd al-Rahman I, Abd al-Rahman II and Al Hakam sectors (b), both drawings adapted from [41].

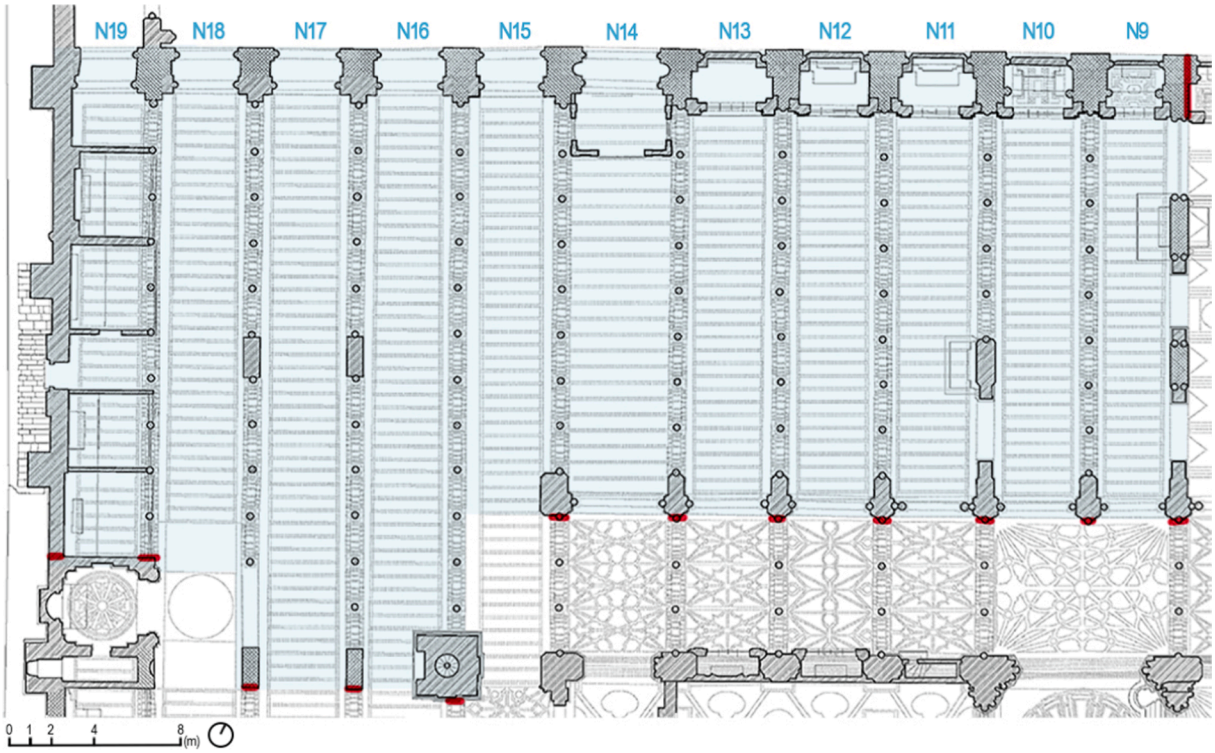

Fig. 5. Plan of the Abd 'al-Rahman I sector, pointing out in red the adjacent sectors (contact sections) and the number of the naves (N_i). This is the nomenclature established by the maintenance plan to refer to the naves of the complex. (For interpretation of the references to colour in this figure legend, the reader is referred to the web version of this article.)

some preliminary results on the compressive strength of the materials (Fig. 8(a)). This is one of the most used NDT to quickly recognise the condition of building structures. Despite being mainly used for concrete elements, specific devices have been developed to evaluate masonry walls, which have been used in the characterisation of old buildings [42]. In this study, two different Schmidt Hammer devices of Proeti SA [43] have been used. They have a rebound energy of 2.207 Nm and a low rebound energy of 0.735 Nm, to specifically obtain the stone and the masonry compressive strength, respectively (Fig. 8(b)).

Fig. 9 shows the identification of the material of the columns as well as the elements tested, which have been highligthed in red. The number of the columns (C_i) has been identified. For each element tested, nine different tests were performed, separated by 10/15 cm. As can be observed, the columns are mainly composed of marble, granite and limestone. The predominant materials of the columns are *Lumachella carnina* marble (53 %), grey granite (21 %) and Estremoz marble from

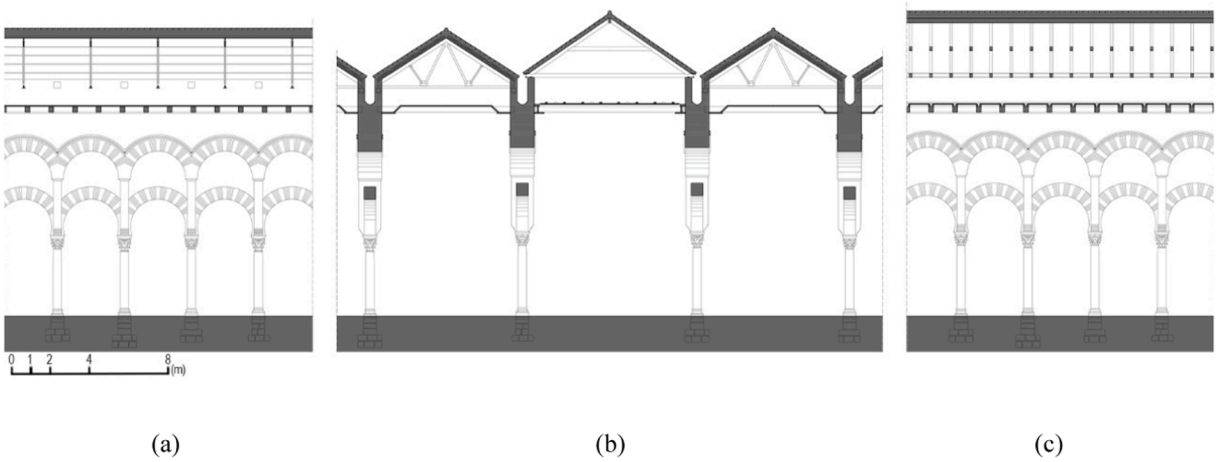

Fig. 6. In detail sections of the Abd 'al-Rahman I sector identifying the type of roof in its current state. (a) Longitudinal section of a nave with the 20th century steel roof; (b) transversal section, being N14 in the centre with timber roofing; (c) longitudinal section of the main nave N14 with the old timber roof. Drawings adapted by the authors from [41], including the foundation.

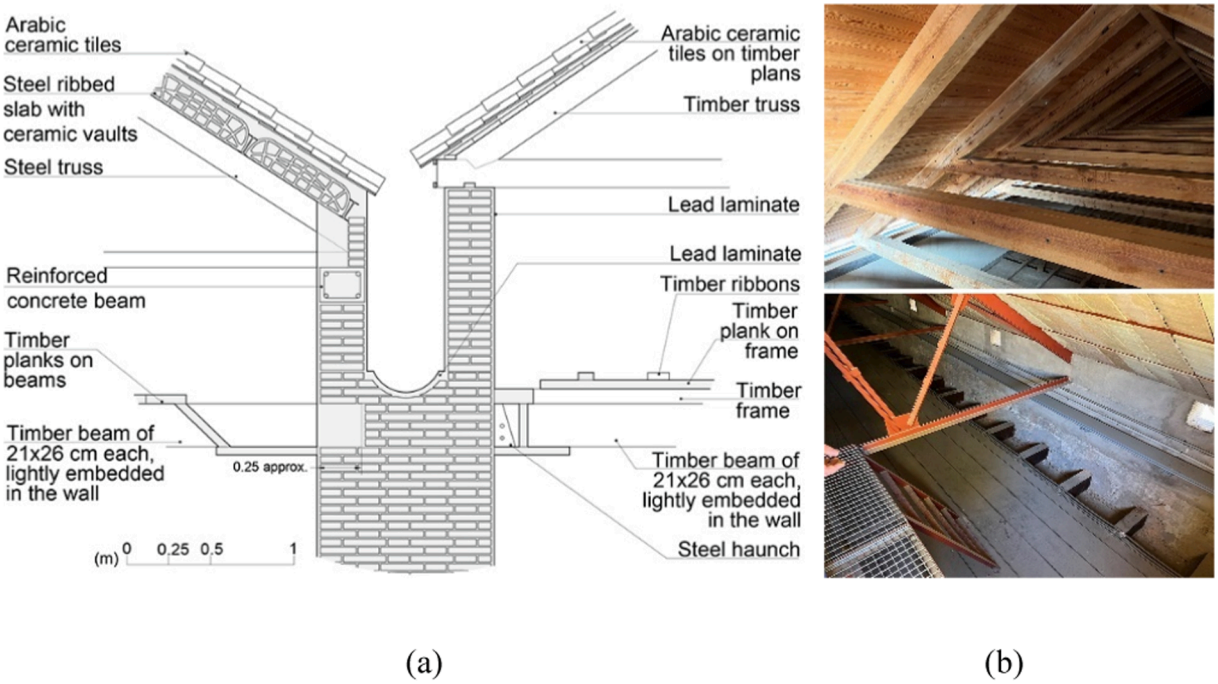

Fig. 7. (a) Detail of the 'aqueducts' that gather the rainwater and support the two different types of roofing. (b) Photographs of the timber and the steel trusses roofing taken by the authors.

Portugal (10.4 %).

Table 1 lists the maximum (max), the minimum (min) and the average (aver) compressive strength (f_c) obtained from the Schmidt Hammer tests on the columns according to the material. Also, the standard deviation (σ) of the test results is provided. In general, the statistics analysis of the samples shows that the results are in good agreement. The results obtained for the Estremoz marble and the violet limestone have been the most disperse. The column made of Antique Nero marble was protected by glass and it could not be tested. In the case of the limestone masonry walls, the results performed on the stone have resulted in values of maximum, minimum and average compressive strength (f_{bc}) of 46 MPa, 22 MPa and 30.20 MPa, respectively, with a $\pm$ 4.7 σ. For the bricks of the vaults and the 'aqueducts', a f_{bc} of 27 MPa with a $\pm$ 1.1 σ has been obtained.

3.2.2. Ambient vibration tests

With the aim of a more reliable modelling and assessment, an OMA has been performed. This is used to identify the overall dynamic behaviour (the natural frequencies and the vibration modes) of the sector and the connection between elements. The dynamic response of the arcades was measured with force-balance triaxial accelerometers, called GMSplus measuring system from GeoSIG Inc (Fig. 10(a)). The sensors are of high sensitivity, reaching an individual low noise of 24-bit $\Delta - \Sigma$ ADC. All the equipment used belongs to the Department of Building Structures and Geotechnical Engineering of the University of Seville. The ARTeMIS Modal software [44] has been used to calculate the frequencies for the later calibration of the numerical model. To do so, and following previous works [20,45], the Enhanced Frequency Domain Decomposition (EFDD) method has been employed.

A surrogate model was firstly created considering some preliminary

(a) (b)

Fig. 8. (a) Performing the Schmidt Hammer test on columns of the sector. (b) Schmidt Hammer devices used for the stone and for the masonry.

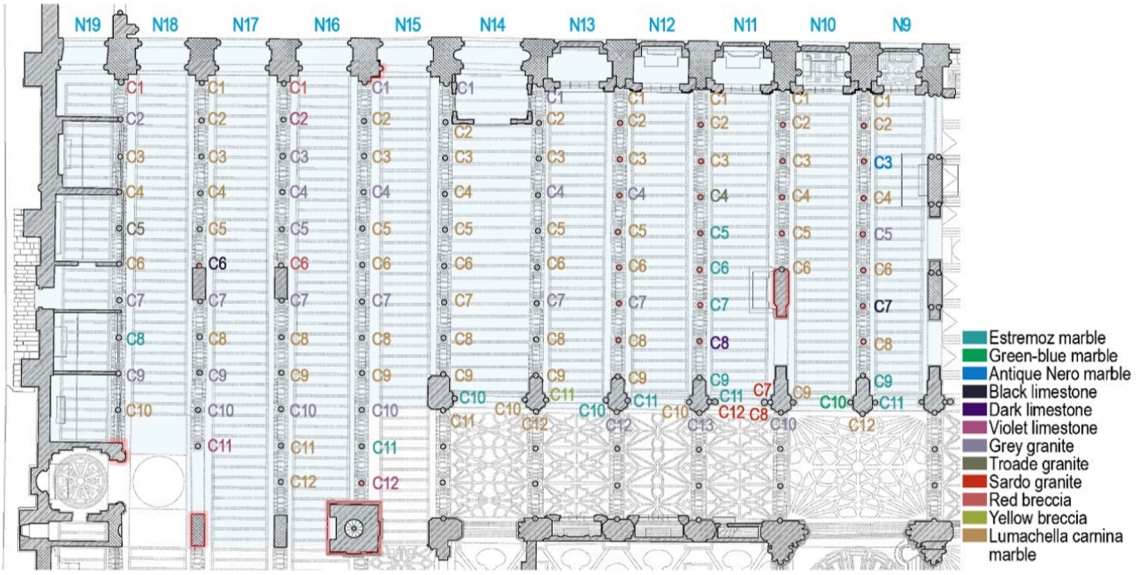

Fig. 9. Plan view of the Abd 'al-Rahman I sector with the identification of the material of the columns and the elements tested (highlighted in red). (For interpretation of the references to colour in this figure legend, the reader is referred to the web version of this article.)

Table 1
Results from the Schmidt Hammer test on the stone materials of the columns.

Material	Group	N°columns	$f_{c,max}$(MPa)	$f_{c,min}$(MPa)	$f_{c,aver}$(MPa)	σ
Lumachella carnina	Marble	61 (53 %)	83.5	50	72	4.5
Estremoz marble	Marble	12 (10.40 %)	80	35	60	8.7
Red *breccia*	Marble	3 (2.60 %)	84	83	83.5	1.5
Green-blue marble	Marble	1 (0.87 %)	75	67	70	5.2
Antique Nero marble	Marble	1 (0.87 %)	–	–	–	–
Yellow *Breccia*	Marble	1 (0.87 %)	82	73	77	4.5
Grey granite	Granite	25 (21.74 %)	80	70	61	5.5
Sargo granite	Granite	3 (2.60 %)	80	80	80	0
Troade granite	Granite	2 (1.74 %)	89	57	77.6	4.3
Violet limestone	Limestone	3 (2.60 %)	89	67	77.8	7.3
Black limestone	Limestone	2 (1.74 %)	80	59	75.5	1.2
Dark limestone	Limestone	1 (0.87 %)	89	64	78	1.7

values obtained from the experimental campaign. The mechanical values considered in this surrogate model are listed in Table 2. This model was used to define the position of the triaxial devices for the free ambient vibration test. To do so, a preliminary modal analysis was performed. The measurement points were located considering the deformed modal shape of each mode of vibration obtained. These were placed in the arcades where they presented a considerable deformation in order to obtain good results while taking the measurement. Two measurements have been performed. First, the global behaviour of the building has been obtained. To do so, the corners of the building have

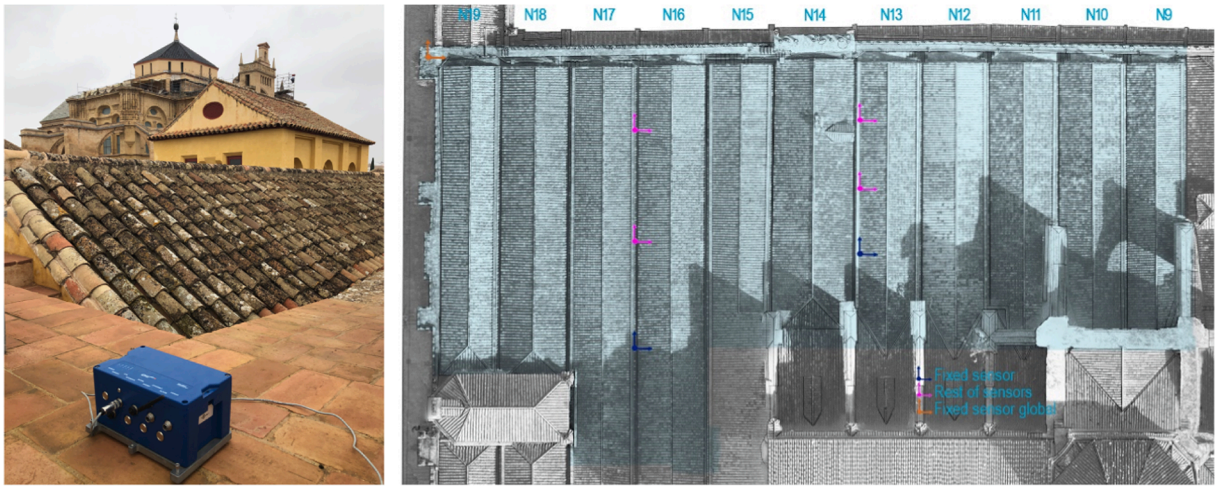

Fig. 10. (a) OMA set-up and (b) location of the accelerometers.

Table 2
Mechanical properties of the materials used in the preliminary analysis.

Material	ρ(T/m^3)	E (GPa)	G (GPa)	ν	f_c(MPa)	f_t(MPa)
Clay bricks and lime mortar masonry	1.8	1.7	0.55	0.2	3.57	0.120
Limestone and lime mortar masonry	1.8	1.7	0.42	0.3	2.78	0.063
Marble	2.8	15	6	0.25	60–83.5	3–4.17
Granite	2.8	35	14	0.25	61–80	3.05–4
Limestone	2.7	10	2	0.25	75.5–78	3.77–3.9
Timber (old roof)	0.45	11	4	0.4	40	10
Steel (new roof)	7.8	210	81	0.3	410	275

been measured (the north-western corner was used as reference). Second, two arcades were assessed to obtain their modal behaviour as individual elements. The vibration modes have been determined by selecting peak values in the response of the spectral density functions of the set of the tests performed. In Fig. 10(b), the layout of the sensors in the arcades is shown, pointing out the reference sensor (in dark blue in a fixed position) and the different measurement points (in pink) considered. The reference-fixed sensor, for the global analysis, has been depicted in orange. The results obtained from the OMA and the calibration of the model have been presented in §5.3. After the OMA, no good results have been obtained for the global analysis. Hence, for the calibration, only the second set of measurements has been considered.

3.2.3. Morphology and mechanical properties

The materials that compose the building are masonry, stone, steel and timber. In this building, masonry walls are either composed of ceramic bricks or limestone and lime mortar. According to the classification on the morphology of masonry [46], the walls are single leaf, where stone and ceramic elements are bound together using mortar. In the case of the stone elements, these are characterised by a regular cut and they are staggered and placed on horizontal courses with thin mortar joints. According to the masonry typologies established in [47], these have been classified as soft stone masonry.

In [48], reference values of soft stone masonry are provided for its mechanical properties: $f_{Mc} = 1.40–2.40$ MPa, $f_{Mt} = 0.042–0.063$ MPa, $E = 900–1700$ MPa, $G = 300–420$ MPa and $\rho = 1.8$ T/m^3. According to the NDT, the average f_{bc} obtained has been 30.2 MPa. According to the EC6 provisions [49], the characteristic compressive strength of stone masonry can be calculated using $f_{M,k} = K f_{bc}^{0.7} f_{mc}^{0.3}$. However, as pointed out in [48], this formulation is proposed for contemporary buildings. Consequently, in the case of old masonry, the value should be modified by a reduction factor of 0.70. For stone ashlar masonry, K is equal to 0.45 and the compressive strength of the lime mortar (f_{mc}) has been defined as 0.5 MPa [48]. As a conclusion, a f_{Mc} equal to 2.78 MPa has been obtained, slightly higher than the reference values.

In the case of the ceramic brick masonry walls, the mortar joints are thick, commonly known as Byzantine brickwork. These walls have been classified as full brick masonry with lime mortar. In [48], reference values of this type of masonry were provided for its mechanical properties: $f_{Mc} = 2.00–4.00$ MPa, $f_{Mt} = 0.040–0.140$ MPa, $E = 240–1800$ MPa, $G = 80–600$ MPa and $\rho = 1.8$ T/m^3. According to the NDT, f_{bc} is 27 MPa. According to the EC6, K is 0.6 for brick work masonry and lime mortar f_{mc} can be considered as 1.5 MPa, resulting in a reduced f_{Mc} equal to 4.76 MPa. Nevertheless, as suggested by [48], the properties of very think mortar joints masonries should be reduced by 0.75, resulting in a f_{Mc} equal to 3.57 MPa, in agreement with the reference values. Considering the values of f_{Mc}, the rest of the parameters have been defined by interpolating the values defined in [48] and paying attention to the following considerations: i) regarding the referenced values of E and G, these relate to the uncracked masonry (it has been checked that E ranges between 200–350f_{Mc}, as suggested by [50]); ii) following the provisions of [48], for uncracked sections, it has been considered that G equals to 1/3–2/5 E as a realistic ration; iii) the f_t is assumed to be equal to 5 % of the compressive strength [1]; iv) the Poisson's ratio has been defined according to [48]. The state of conservation is good and, therefore, no reduction factor for the strength and elastic properties has been considered, as suggested in [51].

For the Mediterranean region, different types of stone units have been defined (depending on their source) and characterised in [48]. According to the NDT campaign, in this building, several stone units have been identified (marble, granite and limestone) and their f_c has been experimentally obtained. It has been checked that the values of f_c, obtained for each unit, have been within the ranges proposed in [52,53]. Hence, the rest of the mechanical properties have been defined considering the values of f_c and interpolating the ranges proposed in these works. These results have been also aligned with the experimental values obtained for another historical building in Andalusia [54]. G has been defined as 0.4E, which is the ratio presented in almost all national building codes. The f_t has been assumed to be, at least, equal to 5 % of f_{Mc}.

The mechanical properties of the old timber roof have been defined according to the experimental results obtained in [55,56]. The new steel trusses added to the roof were S275JR and their mechanical parameters are prescribed by the European regulation.

3.3. Preliminary mechanical parameters

A set of preliminary mechanical parameters has been obtained for each of the materials identified in the sector (Table 2). The procedure followed to define these mechanical values has been: i) performing the NDT campaign (visual inspection and Schmidt Hammer tests) to obtain the type of material, the morphology and the compressive strength; ii) analysing the literature about the characterization of the mechanical properties of those materials; iii) defining the mechanical parameters according to the results obtained in i) by considering ii). These preliminary parameters have been updated later (after the calibration carried out) with the results of the OMA.

4. Performance-based assessment

The performance assessment has been carried out through an NLSA. The use of NLSA for the seismic assessment of historical structures has been proven to be a suitable approach and it is widely documented in the literature [1,12]. For the PBA, the guidelines proposed in [12] have been followed, based on the global scale presented. For this purpose, four PLs have been defined, which are directly correlated with the different damage limits (DL): DL1, no damage; DL2, damage limitation; DL3, significant but repairable damage; and DL4, near collapse. The different DLs have been defined considering the maximum basal shear force (V_b) resisted by the system: DL1 $\geq 0.5V_b$; DL2 $= 0.95V_b$; DL3 $= 0.8V_b$; and DL4 $= 0.7V_b$. Further information on the PBA can be found in [12].

For the demand assessment, the N2-method [57] has been followed, which is the procedure established in the Eurocode-8 part-1 (EC8-1) [58]. As presented in [57], the N2 method combines the multi-degree-of-freedom (MDOF) models with the response spectrum analysis of an equivalent single-degree-of-freedom (SDOF) system. The N2 method is based on the inelastic spectra, which are defined in terms of ductility. As presented in [12], as a preliminary assessment, the N2 method can be considered for the evaluation of the displacement demand on the capacity curve of heritage buildings.

In this case, the seismic capacity is obtained through NLSA while the demand has been defined according to the EC8-1 response spectrum provisions. Following this procedure, the combination of both models results in the commonly known target displacement, i.e., the seismic demand displacement. The peak ground acceleration (PGA) has been adopted as an intensity measure (IM). This has been defined according to the updated values of the Spanish seismic code [59] that states a 0.09 g PGA for Cordoba. This PGA is expressed as a 10 % probability of exceedance, i.e., 475 years of return period. To date, no other values of PGA are expressed for different probabilities of exceedance in the Spanish codes. Nevertheless, as stated in the Eurocode-8 part-3 (EC8-3) [60], this probability of exceedance is correlated to the severe damage limit state, i.e., DL3. Hence, the seismic safety assessment (demand vs damage) has been performed only considering this DL.

5. Numerical modelling

5.1. FE model

The 3D numerical model (Fig. 11(a)) has been developed in the OpenSees framework [61]. Since it is intended to develop an advanced FE modelling, solid elements have been used to create the geometric model in Rhinoceros [62]. As presented in the state of the art, there are several approaches for the modelling of heritage buildings, especially for those composed of masonry walls. The most powerful and adequate for this type of systems is the use of the FE method combined with solid elements. The use of solid elements is time consuming due to the preparation of the model, the calculation time and the analysis of the results. However, FE models with solid elements provide a comprehensive stress–strain behaviour of the elements and the materials (that are often needed for the specific and particular modelling of historical and singular structures [7]). These elements are then combined with the macro-mechanical approach to model the masonry as an isotropic material, as sufficiently proven in [63]. In this work, the FE meshing has been developed in the STKO software [64], a pre- and post-processor for OpenSees. The FE analysis has been performed using the literature data and the NDT results both in terms of geometry and mechanical properties of the materials.

Intention has been paid to preserve, as much as possible, the real configuration, in the analytical model (Fig. 12). Since it is intended to obtain the behaviour of both the light inner and the more massive external elements, the layout has been slightly simplified. To do so, a refined FE mesh has been developed (Fig. 11(b)). The structural intervention of the early 20th century, consisting in changing some damaged

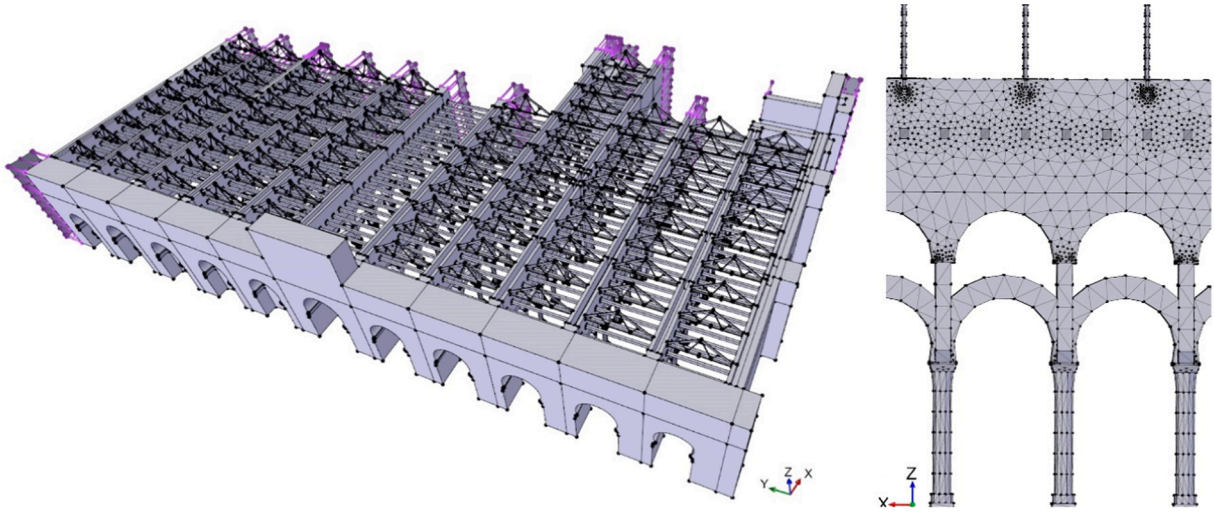

Fig. 11. (a) 3D model developed for the Abd 'al-Rahman I sector. (b) Zoom to the FE-mesh of an arcade, where the tetra-elements can be observed.

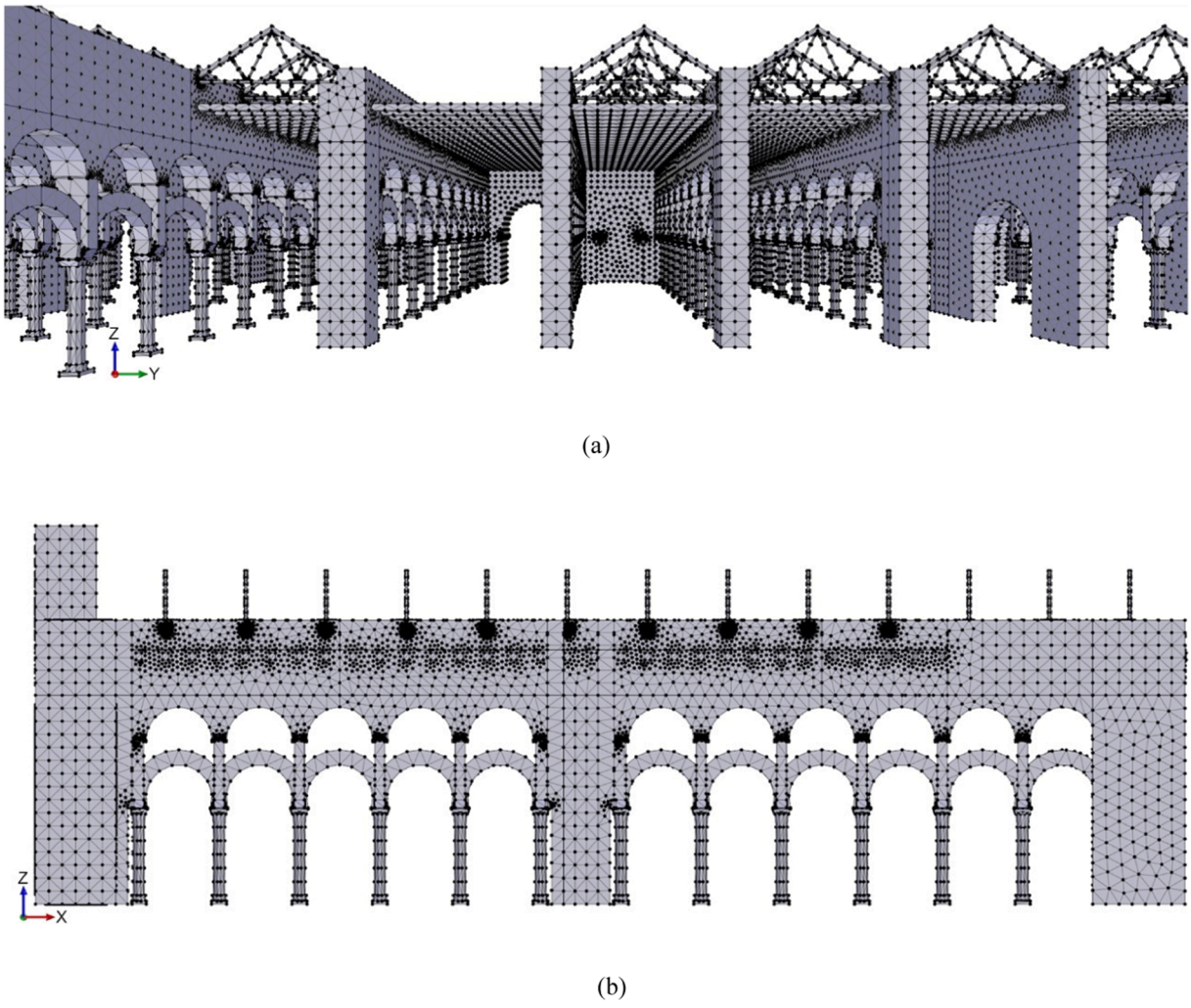

Fig. 12. Transversal (a) and longitudinal (b) views of the 3D FE mesh developed for the Abd 'al-Rahman I sector.

timber trusses for steel ones, has been modelled. The remaining timber trusses have been considered as a simple distributed load, considering the details in Fig. 7. The effect of the rigid diaphragm of the steel roofing has been simulated by means of a constraint between trusses, which has been deleted from the figure to improve its legibility.

As pursued in [1,7,20,65], the mesh size has been defined by obtaining a fair compromise between the computational effort, the accuracy and robustness of the modelling. In this case, the mesh size has been 0.3 m for the walls and, in the columns, it has been set to 0.2 m. These values are similar to those proposed in the works cited. Effort has been made to regularise the mesh to try to use quadratic/hexagonal elements as these elements provide more realistic results [66]. However, owing to the irregularities of this case study, the triangle/tetrahedron elements have had to be used to develop the FE mesh. To do so, the 'FourNodeTetrahedron' solid element from the library of OpenSees has been used. It is a four-node element, with a four-point integration scheme over the volume. To date, this is the only tetra-element available in OpenSees. There are other tetra-elements, such as the 10-point tetrahedron, but they are still under development. Future analyses will be the comparison of the results obtained with both type of tetra-elements. A zoom on the singularities of the mesh using the tetra-element can be seen in Fig. 11(b).

In total, the FE mesh is composed of 1,124,353 tetra-elements and 306,386 nodes. The boundary conditions have been set as fixed constraints at the base of the structure and all the elements of the numerical model have been considered as perfectly connected. As pointed out in [1,67], the connection stiffness is particularly important for the global response of historic structures. In this case, the presence of the adjacent structure has been considered through zero-length 3D contact materials calibrated with the experimental OMA. Further description on the calibration of materials is provided in §5.3.

5.2. Nonlinear behaviour

In this work, the continuous or macro-mechanical approach has been considered to simulate the mechanical behaviour of the structural elements. As highlighted in the state-of-the-art review, this approach has been proved sufficiently efficient and robust method for the modelling of ancient structures. As similar works use, as in this work, a damage-plasticity material, developed within the OpenSees framework, has been employed [68]. This material is typically used to simulate the nonlinear behaviour of quasi-brittle materials such as masonry [39]. As presented in [69], according to the fundamentals of the continuum damage mechanics, it is possible to define the degradation phenomena on a microscale, starting from the initial (undamaged or pre-damaged) state up to the creation of a crack. Hence, the damage may range from $D = 0$ (undamaged material) to the critical value of $D = 1$, which corresponds to entirely damaged material.

The damage-plasticity material implemented presents the same constitutive law and characteristics as other materials implemented in similar works on heritage buildings [39]. Hence, two independent tensile (Fig. 13(a)) and compression (Fig. 13(b)) constitutive laws have

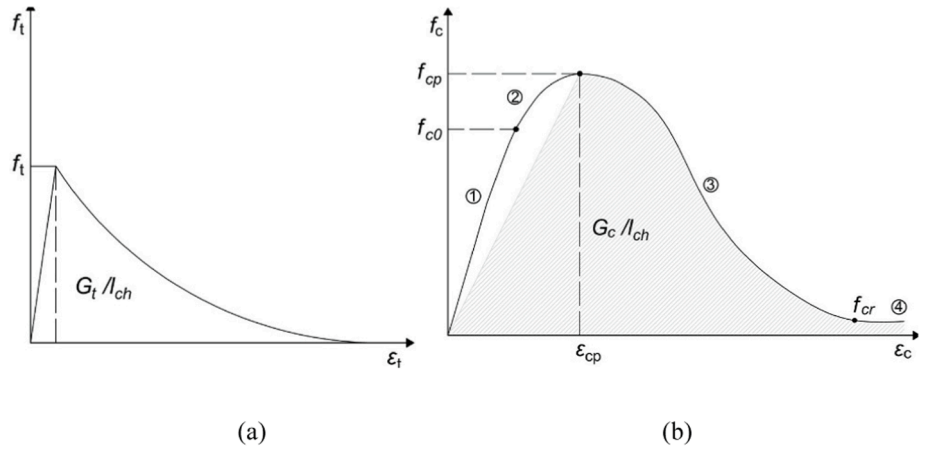

Fig. 13. Tensile (a) and compressive (b) hardening functions adapted from [68].

been defined. For this purpose, the peak (f_{cp}), the elastic (f_{c0}) and the residual (f_{cr}) compressive strengths, as well as the strain (ε_{cp}) at peak compressive strength, are needed. ε_{cp} has been defined considering the values proposed in [47] for each type of material. The tensile constitutive law is defined by means of the peak tensile strength (f_{tp}). Following the prescriptions in [63], f_{c0} and f_{cr} have been defined as $0.8f_{cp}$ and $0.5f_{cp}$, respectively. Under uniaxial tension and compression, the stress–strain follows an elastic relation up to f_{tp} and f_{c0}, respectively. This state corresponds to the micro-cracking of the material. After, in tension, a softening stress–strain response is characterized. However, in the case of compression, the stress–strain presents a plastic range that is typically characterized by stress hardening. Then, it decreases following a softening phase up to an ultimate stress.

For the definition of the fracture energies, the equations proposed in [70] have been used. Hence, the compressive (G_c) and the tensile (G_t) fracture energies have been computed as Eq. (1) and (2), respectively. The input fracture energies have been divided by the element characteristic length (l_{ch}) to obtain a response that is mesh-size independent. The different materials have been defined according to the mechanical characterisation discussed above.

$$G_c = G_t(f_c/f_t)^2 \tag{1}$$

$$G_t = 0.073f_c^{0.18} \tag{2}$$

5.3. Calibration of the numerical models

The calibration of the models is needed to obtain reliable results from the numerical analyses. An iterative process is followed considering the results obtained in the OMA, paying special attention to: the definition of the boundary conditions to account for the influence of the adjacent sectors; the gravitational loads/masses; and the Young's modulus of the materials. There are several advanced procedures for the calibration of numerical models such as those published in [71,72], based on genetic algorithms. In order to use them, several measurements in a certain period of time are needed. In this case, owing to the impossibility of obtaining different measurements, the calibration has been based on the use of the fundamental frequencies and the Mode Complexity Factor (MCF) associated to each mode. Despite its limitations, compared with other advanced calibration methods, it has been used as a first attempt for obtaining the dynamic characterization of the building. Furthermore, this approach has been followed in several works focused on the analysis of heritage buildings [7,20].

Table 3 lists the values of the estimated fundamental frequencies obtained for both arcades in the experimental analysis in ARTeMIS and the numerical model in OpenSees, after the calibration procedure, together with the MCF. This value is scalar and it ranges between 0 % and 100 %. It quantifies the degree of complexity of a mode shape, basically, how much the modal vector differs from a real-valued one [71]. Real-valued mode shapes present complexities close to 0 (MCF-0 %), while mode shapes with mainly imaginary components show complexity values close to 1 (MCF-100 %). In this case, the MCF of each of the experimental modes is lower that 10 %. In both cases, Mode 1 and 3 are translational in the Y (E-W) and X (N-S) directions, respectively. Mode 2 activates vibrations in both directions, being rotational. In Arcade 13–14, higher presence of rotation has been observed reaching a value of rotation in the Z axis of 27.31 %. However, the Arcade 16–17, has presented a rotation value of 8.26 %.

In Fig. 14 and Fig. 15, the deformed shapes obtained experimentally and numerically are shown for each arcade, respectively. The fixed

Table 3
Fundamental frequencies of the arcades considering the OMA and the analytical results.

Arcade	Mode	Direction	ARTeMIS		OpenSees			
			f [Hz]	MCF [%]	f [Hz]	Difference [%]	Mass X [%]	Mass Y [%]
16–17	Mode 1	Translational Y	3.24	3.80	3.13	+3.33	0.002	**24.10**
	Mode 2	Rotational	3.98	8.54	4.13	−3.82	0.004	2.22
	Mode 3	Translational X	7.56	7.52	7.66	−1.36	**74.59**	0.005
	Mode 4	Translational Y	7.85	0.75	7.88	−0.38	0.0002	2.63
	Mode 5	Rotational	10.33	14.90	10.57	−2.23	0.004	0.67
	Mode 6	Rotational	11.08	7.96	10.84	+2.32	0.26	0.95
13–14	Mode 1	Translational Y	2.38	5.75	2.29	+3.78	0.004	**53.75**
	Mode 2	Rotational	4.72	1.09	4.62	+2.26	0.001	1.40
	Mode 3	Translational X	7.802	0.75	7.91	−1.38	**74.36**	0.0001
	Mode 4	Translational Y	10.33	14.90	10.64	−3.00	0.001	5.55
	Mode 5	Rotational	11.08	7.96	10.70	+3.43	0.000	5.71
	Mode 6	Rotational	13.34	12.19	12.58	+5.70	0.0004	0.90

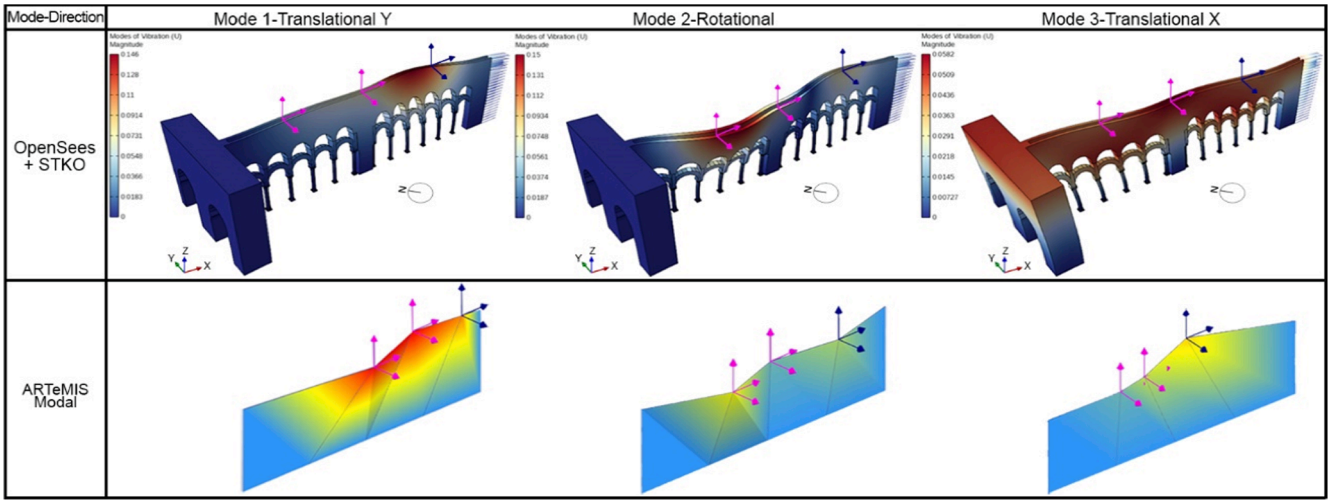

Fig. 14. Mode shape of the arcade 16–17, considering the OMA and the analytical results.

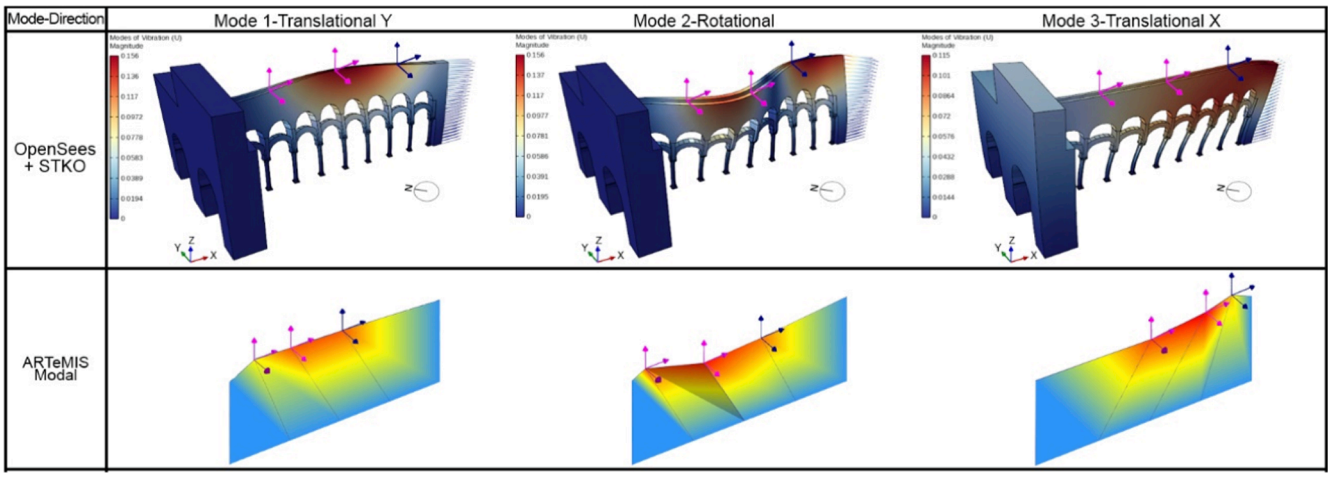

Fig. 15. Mode shape of the arcade 13–14, considering the OMA and the analytical results.

(blue) and the measurement (pink) sensors are pointed out in both cases. After the calibration, as can be noted, the relative error between the frequencies from both analyses is very similar. Table 4 lists the final values of the mechanical parameters after the calibration.

To simulate the presence of the adjacent sectors, zero-length 3D contact materials have been used. Hence, the node-to-node 'ZeroLengthContact' element, available in the OpenSees library, has been used. The contact forces are meant to follow a classical Mohr-Coulomb criterion as in [73]: $T = \mu N + c$, where T is the tangential force and N is the normal force across the interface. μ is the friction coefficient and c is the total cohesion (summed over the effective area of contact nodes).

Table 4
Mechanical properties of the materials defined after the calibration.

Material	ρ(T/m^3)	E (GPa)	G (GPa)	ν	f_c(MPa)	f_t(MPa)
Clay bricks and lime mortar masonry	1.8	2.0	0.55	0.2	3.57	0.21
Limestone and lime mortar masonry	1.8	1.8	0.42	0.3	2.78	0.10
Marble	2.8	16	6	0.25	60–83.5	3–4.17
Granite	2.8	42	14	0.25	61–80	3.05–4
Limestone	2.7	10	2	0.25	75.5–78	3.77–3.9
Timber (old roof)	0.45	11	4	0.4	40	10
Steel (new roof)	78	210	81	0.3	410	275

In this work, no specific tests on the existing masonry have been caried out to provide more detailed information. Hence, in this case, the values needed to define the contact elements for the numerical model have been adopted from literature. These later were calibrated with the OMA results. However, the authors would like to point out the uncertainties in this procedure and the need to perform specific analyses on the mechanical properties of the masonry.

In this case, the contact is located between masonry elements. As pointed out in [73], the friction coefficient assumes values ranging from 0.3 to simulate very poor mortar and 0.5 for good quality of mortar in the masonry walls. In this case study, the masonry pattern is quite regular and presents quite a good quality, hence, a standard value of $\mu = 0.5$ has been considered. As suggested in [48], for old brick masonry, the cohesion should range in the range of 0.05–0.1 MPa. In this case, a value of 0.1 MPa is considered, since the masonry (both brick and mortar) presents good quality. This is also in agreement with [66]. The values of the stiffness in the normal (Kn) and the tangential (Kt) direction have been defined according to [73] and varied to calibrate the model. The final values obtained are 2e + 9 and 6e + 8 kPa/m for Kn and Kt, respectively.

6. Preliminary analyses and results

After the calibration of the model, the modal analysis and a set of

NLSA, considering gravitational and horizontal (pushover) loads, have been performed on the complete sector. Both NLSA are based on an incremental-iterative method, using a constant gravitational and a monotonically increased horizontal load, respectively. The gravitational analysis has been performed by means of a load-control integrator. The horizontal analysis has been carried out through a displacement-control integrator. Similar characteristics for the set-up of the analyses have been defined. The Penalty method has been considered to handle the constraints. The Penalty method consists of adding large numbers to the stiffness matrix and restoring the force vectors to impose a prescribed displacement or nonzero degree-of-freedom. As suggested in the literature, the choice of the penalty parameters should be done accurately and, if possible, in comparison with another handler. The highest stiffness order of magnitude in the model should be incremented up to 8 (with particular attention to the units). The Parallel RCM numberer, the Krylov-Newton algorithm and the Mumps system have been used. A normalised displacement increment has been defined with a tolerance of 10E-4. An AMD Ryzen 9 3900 12-Core Processor has been used for the analyses and the model has been divided into 24 partitions, performing the NLSA in around 60 min.

6.1. Modal analysis

In Fig. 16, the global shapes of the first three principal modal modes are shown. As can be seen, the Mode 1 and Mode 2 are translational in X (N-S) and Y (E-W), respectively. The modal participation factors are 26 % and 40 %. Mode 3 is rotational. The values of the periods of these first three modes are 0.23 s, 0.22 s and 0.18 s. With the modal analysis, in OpenSees, the total mass of the system has been calculated, obtaining a total value of 11,849 T.

6.2. Gravitational nonlinear analysis

The gravitational loads have been applied in the structural elements as volume forces (command available in OpenSees), considering the density of the materials. In Fig. 17, the damage pattern in tension (d^+) and in compression (d^-) is presented after the application of the self-weight of the structural elements. The damage in the structural elements ranges from 0 to 1, being 0 non-damaged and 1 damaged. As can be observed, no elements are damaged after the application of the gravitational loads, which is the actual situation of the asset as discussed in §3.1. Particular attention should be paid to the cymatiums (Fig. 18). As can be noted, in these parts, the damage reaches values close to 0.7 and 0.9 in compression and tension, respectively. This can be due to the actual configuration of the double honeycomb arcades. The cymatiums concentrate the vertical loads from the arches into the columns, which in turn are the most demanded parts. Damage in tension ranging from 0.3 to 0.5 is also seen in the support of the roofing.

6.3. Horizontal nonlinear static analysis

Codes usually propose to assume at least two load patterns. This is due to the re-distribution of the inertial force changes: as damage increases, the inertial forces distribution changes from a modal to a uniform one. In this work, it has been opted to perform the pushover analyses considering only a uniform load pattern. This has been done in agreement to [37], where the authors show that the modal pattern is not reliable in the case of flexible horizontal diaphragms (which are typical in heritage buildings such as the Mosque-Cathedral of Cordoba). This is due to the fact that each mode involves the local behaviour of single walls, having an outstanding contribution in the participating mass. Furthermore, the uniform load pattern is generally accepted by the EC8-3 to perform a preliminary NLSA on heritage buildings, as suggested in [1,12]. The loads are applied along the two main directions of the building, X (N-S) and Y (E-W), for both the positive and the negative orientations. The ultimate displacement is calculated following the prescriptions established in [20] and in the EC8. Subsequently, this displacement is considered as 20 % of the decay of the pushover curve, i.e., $0.8V_b$. This value corresponds to DL3, according to the guidelines in [12], which represents the usability prevent DL. Therefore, safety is referred to this DL3.

Fig. 19 shows the resulting pushover curves obtained in terms of a load factor (total base shear divided by the weight (W) of the structure) and the displacement of the control node located at the top. As pointed out in the state-of-the-art review, the choice of the control node is highly important to optimize the convergence of the NLSA [37]. Regarding its elevation, codes usually propose to assume the control node at the top floor, above the level in which the collapse occurs. Concerning the in-plain position, this choice is crucial, especially in buildings with timber floors (with flexible diaphragms). In this type of buildings (such as

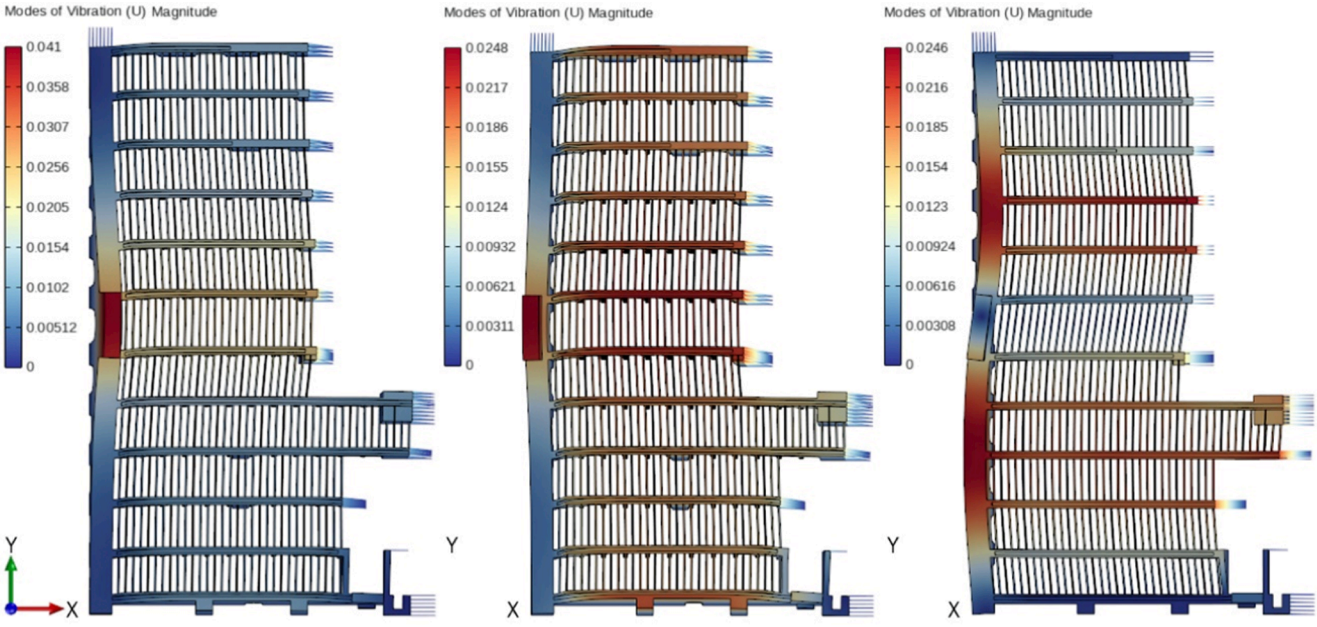

Fig. 16. Global modal shapes 1, 2 and 3 of the Abd 'al-Rahman I sector.

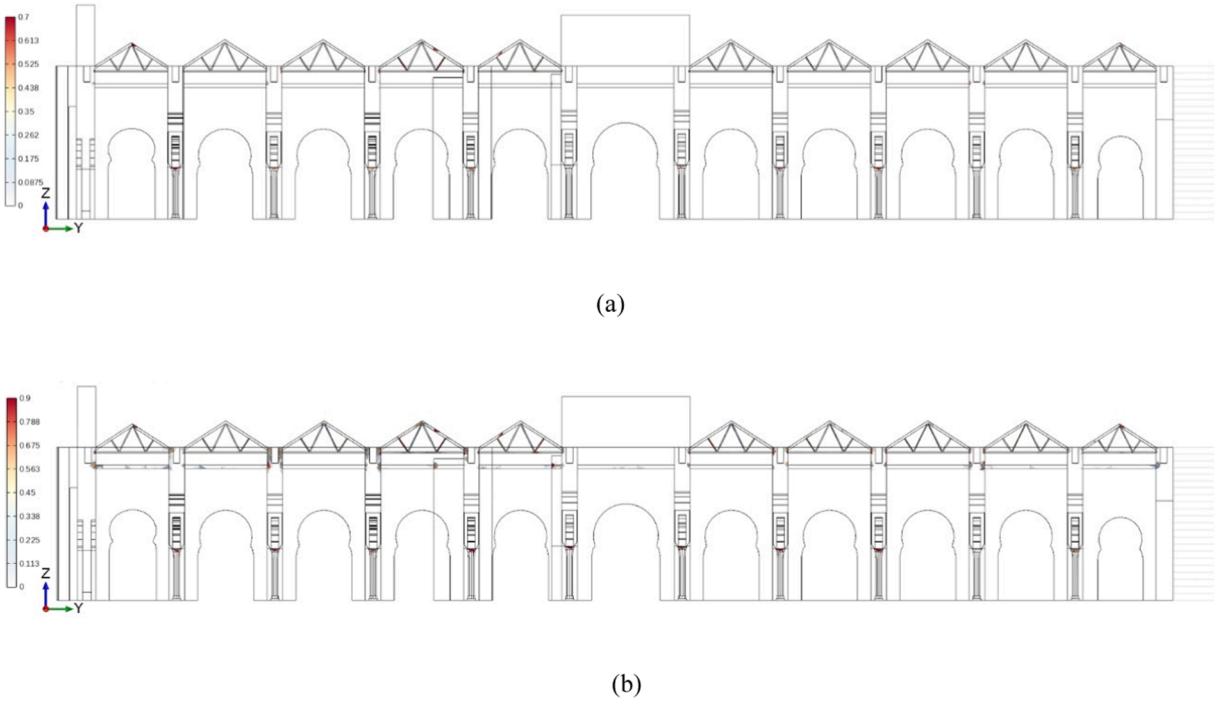

Fig. 17. Material damage in compression (d^-) (a) and tension (d^+) (b) due to the application of the gravitational loads.

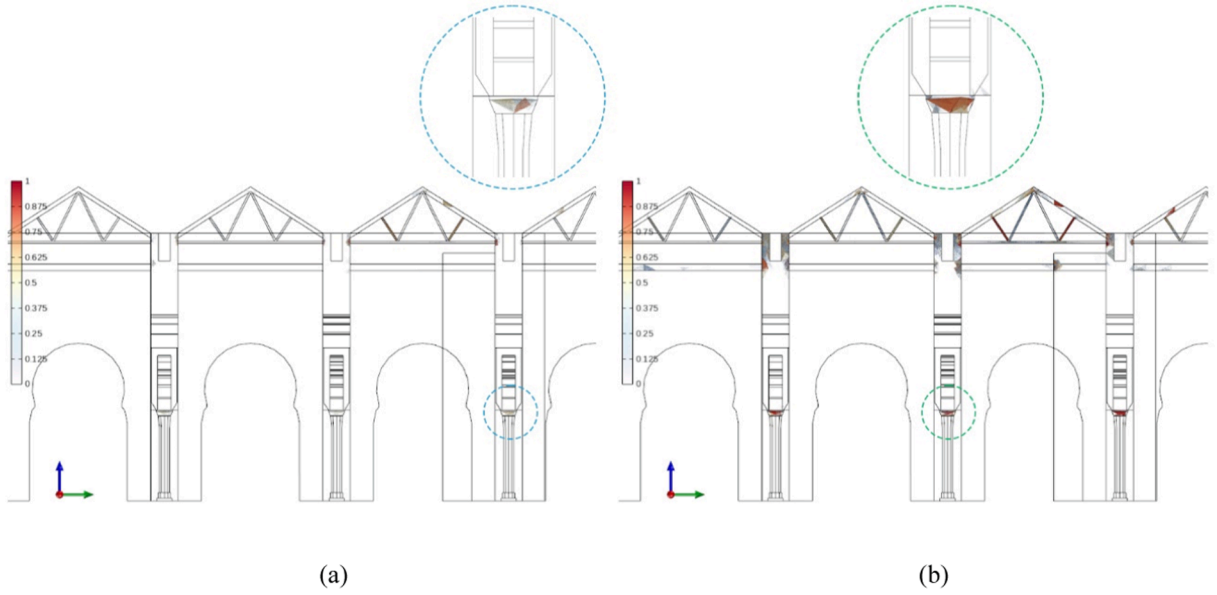

Fig. 18. Zoom to the material damage in compression (d^-) (a) and tension (d^+) (b) due to the application of the gravitational loads.

the case study), the control node strongly depends on the different stiffness and strength of the masonry walls. In this work, the control node has been located in the centre of the masses of the structure, which has been automatically obtained after the global modal analysis. This position is generally selected when assessing heritage structures, as established in similar works [1,12,20]. As can be seen in Fig. 19, the initial stiffness of the curves are similar up to a displacement corresponding to around 1 cm in the positive direction and slightly lower in the negative one. This is due to the application of the loads, which have been applied on the external walls. Since these are composed of the same materials and they have a similar thickness, the behaviour of the system at the earlier steps of the analysis is rather similar. After that, it can be seen that in the X (N-S) direction, the system presents a higher resistance compared to the Y direction. This is mainly due to the bracing effects that the arcades generate in the X direction. Similar curves have been obtained for the positive and the negative orientation in the X direction. Nevertheless, in the Y direction, a significant decay of the curve can be observed in the -Y direction, resulting from the different value of the initial stiffness. A sensitivity analysis on the position of the control node has been carried out, resulting in similar values for the pushover curves. Hence, in this case, the most vulnerable curves have been plotted, which have been obtained for a control node located on the centre of the masses of the system. It has been checked that the results obtained are in agreement with the peak strength and the displacement corresponding to this type of structural configuration and period of construction, as obtained in [7,18,30].

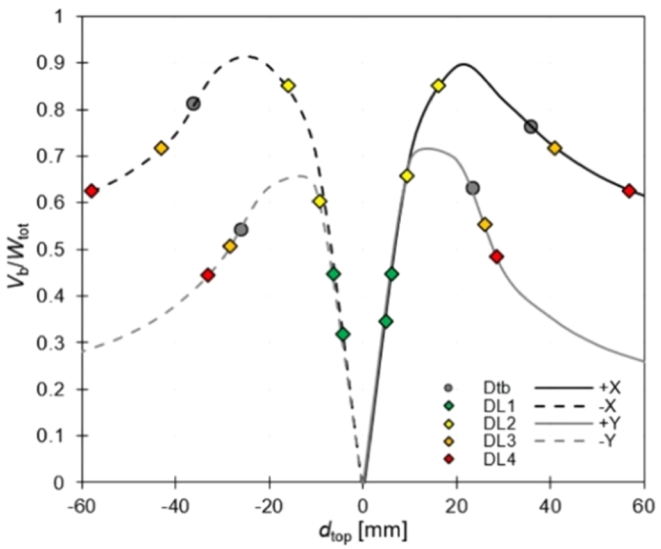

Fig. 19. Capacity curves obtained in the NLSA.

6.4. Damage assessment

Considering the DLs computed for each global curve (Fig. 19), it can be seen that for the seismic demand displacement (d_{tb}), the PL expected is limited in both directions, ranging between DL2-DL3. As presented in [12], this level of damage means that some parts of the building might be slightly damaged but could be easily repaired. Particularly, in the case of the Y-direction, since the behaviour is slightly worse than in the X-direction, the seismic demand is closer to the DL3. The safety verification has been checked following the EC8-3 prescription. According to this, the ration between the DL3 and the seismic demand displacements d_{DL3}/d_{tb} should be higher than 1. In this case, it has been obtained that for the +X-direction, it is 1.14 and for the +Y-direction, it is 1.11.

Detailed meshing models with the concentration of the damage and the possible crack patterns are discussed. These have been plotted for the two principal directions of the building and for the pushover step when the d_{tb} is attained in each direction. In Fig. 20, the damage concentration for the +X direction is shown in tension (a) and in compression (b). As can be observed, for the tension, the damage is mainly concentrated in the low part of the north wall, reaching values close to 1 (completely damaged). In the highest part of this wall, some cracks could also appear. Nevertheless, the highest values of damage can be found in the contact between the north wall and the arcades. This can be due to the different materials that compose both walls: limestone and ceramic bricks masonry for the perimeter and inner walls, respectively. Furthermore, the horizontal connection between both walls could not be completely rigid. As seen in Fig. 21, additional damage in tension es expected in the first row of the arches of all the arcades. Also, excessive damage in tension is expected at the low parts of the columns shafts and bases.

In the case of the compression, no excessive damage has been seen apart from a few cymatiums being excessively demanded and some parts of the arches, as seen in Fig. 21. However, in the contact between the north wall and the arcades, significant damage is expected, reaching values close to 0.8–0.9. Hence, bearing in mind the excessive damage obtained in tension, this contact can be considered as one of the weakest parts of the structural system. This is in agreement with the historical records of the reinforcements carried out in this wall.

In Fig. 22, the damage concentration for the +Y direction is shown in tension and in compression. As can be seen, the damage expected is higher in this direction compared to the other one. As previously commented, this can be due to the bracing effect of the arcades in the other direction. In this case, for the tension, the western wall would be significantly damaged, presenting more parts with excessive damage than the north wall. Damage is concentrated in the lower parts and, to some extent, in the upper part. Similarly to the X direction, a significant damage is also concentrated in the contact between the north wall and the arcades (Fig. 23). Also, as seen in Fig. 23, in tension, the cymatiums are expected to present excessive damage. In the case of compression, no excessive damage is observed since just the north-western wall is expected to be damaged in the upper part.

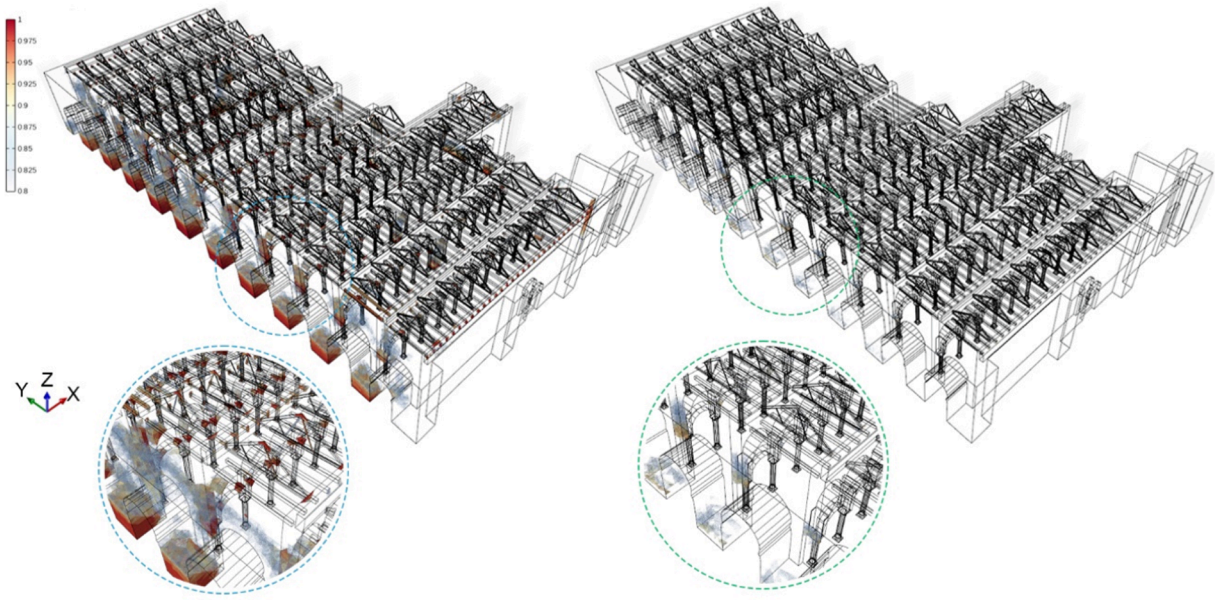

Fig. 20. Damage pattern for the +X direction in tension (a) and in compression (b).

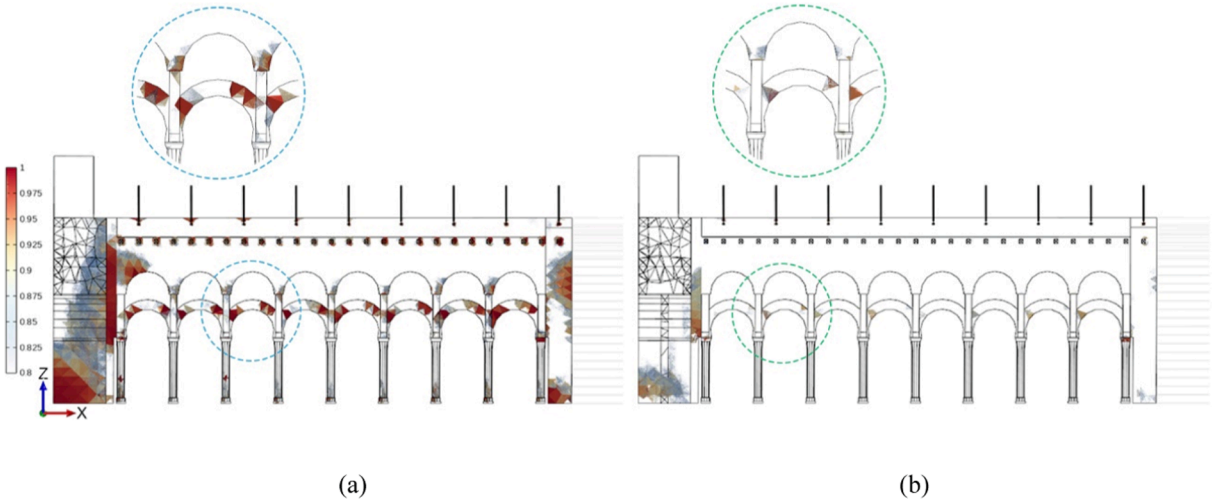

Fig. 21. Lateral view of the damage pattern for the +X direction in tension (a) and in compression (b).

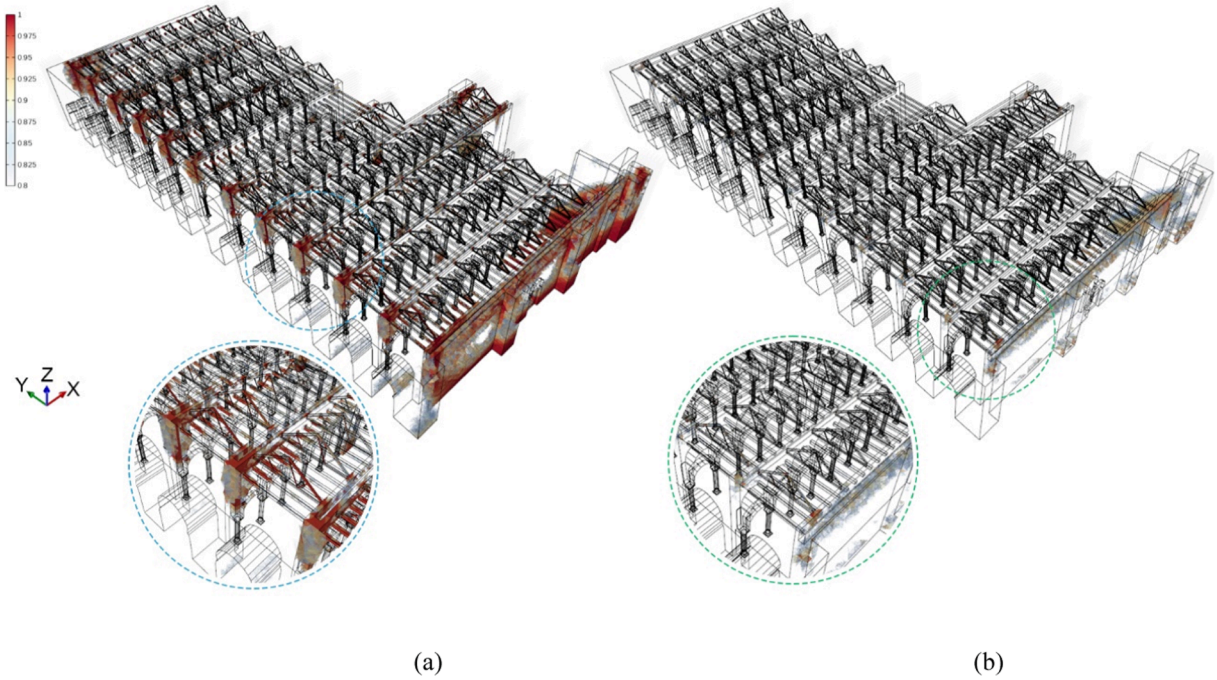

Fig. 22. Damage pattern for the +Y direction in tension (a) and in compression (b).

7. Conclusions and future developments

This paper has addressed the preliminary structural and the seismic assessment of the Mosque-Cathedral of Cordoba, located in the Spanish earthquake-prone region of Andalusia. The UNESCO declared this building as a World Heritage Site of Outstanding Value due to its historic, architectural and artistic value. Given the complexity of the asset, this work has focused on the assessment of the Abd al-Rahman I sector, which is the oldest part of the complex, dating from the 8th century.

A comprehensive investigation for the structural and the seismic assessment of the sector has been performed. Refined macro-modelling FE-based models have been calibrated through an experimental campaign based on NDT and the available data to obtain the behaviour and the dynamic characteristics of the asset (frequencies and modes of vibration). Quasi-static analyses have been performed, based on gravitational and horizontal load patterns. This has allowed obtaining the damage and the crack patterns. Also, its seismic safety has been assessed.

Particularly, this work has drawn some conclusions:

- The OMA has allowed calibrating the numerical model, obtaining, at the end of the iterative procedure, relative errors between frequencies of ± 3.8 %.
- Generally, the numerical damage for the gravitational load pattern seems in good agreement with the data collected from the in situ survey. It was obtained that particular attention should be paid to the cymatiums, since the damage in compression and in tension reaches values close to 0.7 and 0.9, respectively.
- Pushover analyses resulted in a different capacity for the +X and +Y directions of the building. In this case, the building presents a higher capacity in the +X direction, which might be due to the bracing effects of the arcades. A sensitivity analysis on the position of the control node was performed. It was concluded that the most vulnerable curves are those obtained for a control node located in the centre of masses of the building.

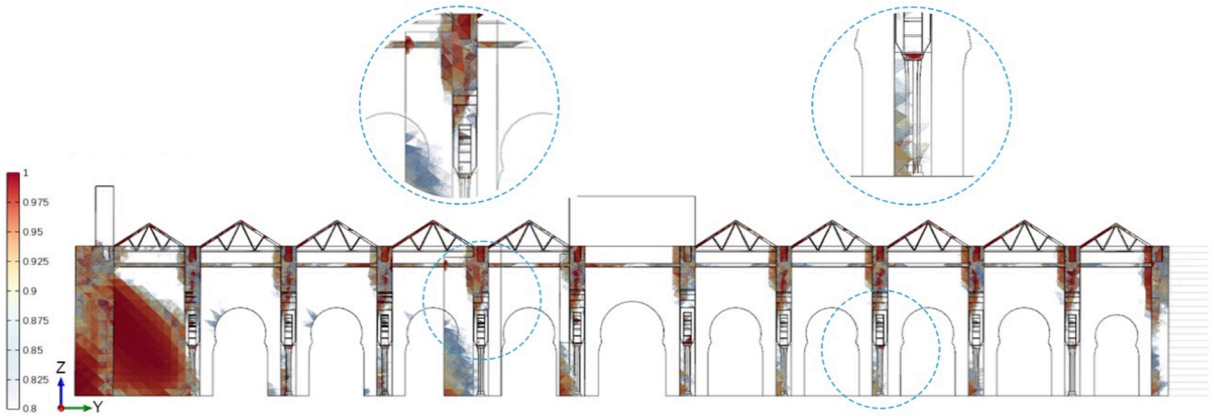

Fig. 23. Lateral view of the damage pattern for the +Y direction in tension.

- It has been established that the PL of the sector is expected in both directions to range between DL2-DL3. Hence, for the seismic demand, light damage is expected, but it could be easily repaired. According to the prescriptions of the EC8, it has been found that the seismic safety is satisfied considering the ground acceleration prescribed by the current Spanish seismic code. It should be highlighted that the worst results were obtained for the +Y-direction.
- For the seismic demand, damage in tension is expected to be concentrated in the contact between the arcades and the north wall for both principal directions. Additional damage in tension is expected in the first row of arches of all the arcades.

Given the recent historiography of the Mosque-Cathedral of Cordoba, pointed out in the state of the art, this work expands the study of its features to the structural and the seismic analysis. The main novelties of this work are:

- Studying the structural features of this building for the first time with advanced methods.
- Developing a methodology in the OpenSees framework based on FE analysis, macro-mechanical modelling and experimental results for the validation of the analytical model. To the authors' knowledge (after an exhaustive review of the literature), this is the first time that a macro-modelling approach with solid elements is presented for the seismic assessment of heritage buildings using the OpenSees framework.
- Performing NDT on a masterpiece building that had not been done to date. These have allowed identifying the materials and the mechanical properties of the structural elements as well as the dynamic behaviour the system.
- Obtaining some preliminary results that can be used in future research works but also for practitioners, especially for the maintenance workers.
- Obtaining the structural behaviour of a specific structural configuration (the double horse-shoe arch) and identifying the weakest elements of a mosque-like building.
- According to the results obtained, both the internal damage and the cracking pattern of the building have been depicted.

This study shows how advanced numerical analyses can provide useful information to assess the existing damage on monumental buildings. Also, this work aims at contributing to the assessment of the vulnerability and the safety of one of the most emblematic mosque-like buildings of the world. This work represents the first attempt to study the structural and the seismic performance of the Mosque-Cathedral of Cordoba using advanced numerical modelling. It has allowed to draw some preliminary results and conclusions. However, as seen, this is a very complex building and, therefore, more specific and exhaustive studies are needed to properly assess the structural and seismic behaviour. Despite its feasibility and simplicity, as discussed in this research, NLSA present several limitations and simplifications for heritage building. Therefore, as a continuation of this work, in the near future, the authors are encouraged to develop dynamic analyses, such as time-history or incremental dynamic analysis. Also, in this work, the macro-mechanical modelling approach is used. However, as concluded in [74], in ancient building, the stereotomy has greatly influenced the dynamic response of ancient masonry structures. Therefore, a discrete-element behaviour assessment can be of great interest to provide some insight on the specific behaviour of this mosque-like configuration. Finally, special interest is also taken by the authors in the specific study of the effects of the soil structure-interaction in the building [75,76].

CRediT authorship contribution statement

M.V. Requena-Garcia-Cruz: Conceptualization, Methodology, Data curation, Investigation, Formal analysis, Software, Validation, Writing – original draft, Writing – review & editing. **E. Romero-Sánchez:** Methodology, Investigation, Software, Validation, Writing – review & editing. **M.P. López-Piña:** Software, Validation. **A. Morales-Esteban:** Conceptualization, Supervision, Writing – review & editing, Funding acquisition, Project administration.

Declaration of Competing Interest

The authors declare that they have no known competing financial interests or personal relationships that could have appeared to influence the work reported in this paper.

Data availability

Data will be made available on request.

Acknowledgements

This work has been supported by the "Fondo Europeo de Desarrollo Regional" FEDER_US-1380730 project. The authors would like to thank the Cathedral of Cordoba's Chapter for the support and for enabling the study of the monument. Specially, we would like to thank Prof. Gabriel Rebollo Puig, the architect in charge of the building, for his support and willingness to help. The funding provided by the *Instituto Universitario de Arquitectura y Ciencias de la Construcción* is also acknowledged. Also, the help provided by Dr. Enrique Vázquez and Dr. Álvaro Serrano with the OMA analysis is acknowledged.

References

[1] Vuoto A, Ortega J, Lourenço PB, Javier Suárez F, Claudia Núñez A. Safety assessment of the Torre de la Vela in la Alhambra, Granada, Spain: the role of on site works. Eng Struct. 2022;264. https://doi.org/10.1016/J.ENGSTRUCT.2022.114443.

[2] Word Heritage Committee. United Nations Educational, Inscription: The Mosque of Cordoba (Spain) (08COM IXA), in: Convention Concerning the Protection of the World Cultural and Natural Heritage, 1984.

[3] Cantizani-Oliva J, Reinoso-Gordo J-F, Gámiz-Gordo A. Proportions and Deformations in the Mosque-Cathedral of Cordoba. Nexus Netw J 2022;2022:1–21. https://doi.org/10.1007/S00004-022-00622-Y.

[4] Ortiz-Cordero R, León Pastor E, Hidalgo Fernández RE. Proposal for the improvement and modification in the scale of evidence for virtual reconstruction of the cultural heritage: A first approach in the mosque-cathedral and the fluvial landscape of Cordoba. J Cult Herit 2018;30:10–5. https://doi.org/10.1016/j.culher.2017.10.006.

[5] Hidalgo Fernández RE, Ortiz-Cordero R. The Mosque-Cathedral of Córdoba: Evidence of column organization during their first construction s. VIII A.D. J Cult Herit 2020;45:215–20. https://doi.org/10.1016/j.culher.2020.05.011.

[6] Suárez R, Alonso A, Sendra JJ. Virtual acoustic environment reconstruction of the hypostyle mosque of Cordoba. Appl Acoust 2018;140:214–24. https://doi.org/10.1016/J.APACOUST.2018.06.006.

[7] Dinani AT, Bisol GD, Ortega J, Lourenço PB. Structural Performance of the Esfahan Shah Mosque. J Struct Eng 2021;147:05021006. https://doi.org/10.1061/(ASCE)ST.1943-541X.0003108.

[8] Fazendeiro Sá L, Morales-Esteban A, Durand P. A Seismic Risk Simulator for Iberia. Bull Seismol Soc Am 2016;106:1198–209. https://doi.org/10.1785/0120150195.

[9] Amaro-Mellado JL, Morales-Esteban A, Asencio-Cortés G, Martínez-Álvarez F. Comparing seismic parameters for different source zone models in the Iberian Peninsula. Tectonophysics 2017;717:449–72. https://doi.org/10.1016/J.TECTO.2017.08.032.

[10] Amaro-Mellado JL, Morales-Esteban A, Martínez-Álvarez F. Mapping of seismic parameters of the Iberian Peninsula by means of a geographic information system. Cent Eur J Oper Res 2017. https://doi.org/10.1007/s10100-017-0506-7.

[11] Romero Sánchez E, Morales Esteban A, Requena García de la Cruz MV, Navarro Casas J. Analysis of the giralda tower geotechnical profile and its settlements. Int J Comput Methods Exp Measur 2022;10:1–12. https://doi.org/10.2495/CMEM-V10-N1-1-12.

[12] Lagomarsino S, Cattari S. PERPETUATE guidelines for seismic performance-based assessment of cultural heritage masonry structures. Bull Earthq Eng 2015;13:13–47. https://doi.org/10.1007/s10518-014-9674-1.

[13] Requena-Garcia-Cruz MV, Morales-Esteban A, Durand-Neyra P. Optimal ductility enhancement of RC framed buildings considering different non-invasive retrofitting techniques. Eng Struct 2021;242:112572. https://doi.org/10.1016/j.engstruct.2021.112572.

[14] Requena-García-Cruz MV, Morales-Esteban A, Durand-Neyra P, Estêvão JMC. An index-based method for evaluating seismic retrofitting techniques. Application to a reinforced concrete primary school in Huelva. PLoS One 2019;14:e0215120.

[15] Bento R. Analysis Case Studies in Evaluation, Rehabilitation and Reconstruction of the Built Heritage. In: European Conference on Earthquake Engineering and Seismology; 2022. p. 245–60. https://doi.org/10.1007/978-3-031-15104-0_15.

[16] Cattari S, Calderoni B, Calìò I, Camata G, de Miranda S, Magenes G, et al. Nonlinear modeling of the seismic response of masonry structures: critical review and open issues towards engineering practice. Bull Earthq Eng 2022;20:1939–97. https://doi.org/10.1007/S10518-021-01263-1.

[17] Rossi M, Cattari S, Lagomarsino S. Performance-based assessment of the Great Mosque of Algiers. Bull Earthq Eng 2015;13:369–88. https://doi.org/10.1007/s10518-014-9682-1.

[18] Portioli F, Mammana O, Landolfo R, Mazzolani FM, Krstevska L, Tashkov L, et al. Seismic Retrofitting of Mustafa Pasha Mosque in Skopje: Finite Element Analysis. J Earthq Eng 2011;15:620–39. https://doi.org/10.1080/13632469.2010.532580.

[19] Requena-García-Cruz MV, Cattari S, Bento R, Morales-Esteban A. Comparative study of alternative equivalent frame approaches for the seismic assessment of masonry buildings in OpenSees. J Build Eng 2023;105877. https://doi.org/10.1016/j.jobe.2023.105877.

[20] Malcata M, Ponte M, Tiberti S, Bento R, Milani G. Failure analysis of a Portuguese cultural heritage masterpiece: Bonet building in Sintra. Eng Fail Anal 2020;115. https://doi.org/10.1016/J.ENGFAILANAL.2020.104636.

[21] Clementi F. Failure Analysis of Apennine Masonry Churches Severely Damaged during the 2016 Central Italy Seismic Sequence. Buildings 2021;11:58. https://doi.org/10.3390/buildings11020058.

[22] Schiavoni M, Giordano E, Roscini F, Clementi F. Numerical Assessment of Interacting Structural Units on the Seismic Damage: A Comparative Analysis with Different Modeling Approaches. Appl Sci 2023;13:972. https://doi.org/10.3390/app13020972.

[23] D'Altri AM, Sarhosis V, Milani G, Rots J, Cattari S, Lagomarsino S, et al. Modeling Strategies for the Computational Analysis of Unreinforced Masonry Structures: Review and Classification. Arch Comput Meth Eng 2020;27:1153–85. https://doi.org/10.1007/s11831-019-09351-x.

[24] Chiorino MA, Spadafora A, Calderini C, Lagomarsino S. Modeling Strategies for the World's Largest Elliptical Dome at Vicoforte, International Journal of. Archit Herit 2008;2:274–303. https://doi.org/10.1080/15583050802063618.

[25] Bartoli G, Betti M, Borri C. Numerical Modeling of the Structural Behavior of Brunelleschi's Dome of Santa Maria del Fiore, International Journal of. Archit Herit 2015;9:408–29. https://doi.org/10.1080/15583058.2013.797038.

[26] Bacigalupo A, Brencich A, Gambarotta L. A simplified assessment of the dome and drum of the Basilica of S. Maria Assunta in Carignano in Genoa. Eng Struct 2013;56:749–65. https://doi.org/10.1016/j.engstruct.2013.05.006.

[27] Milani G, Clementi F. Advanced Seismic Assessment of Four Masonry Bell Towers in Italy after Operational Modal Analysis (OMA) Identification. Int J Archit Herit 2021;15:157–86. https://doi.org/10.1080/15583058.2019.1697768.

[28] Valente M. Seismic vulnerability assessment and earthquake response of slender historical masonry bell towers in South-East Lombardia. Eng Fail Anal 2021;129:105656. https://doi.org/10.1016/j.engfailanal.2021.105656.

[29] Valente M, Milani G. Seismic response and damage patterns of masonry churches: Seven case studies in Ferrara, Italy. Eng Struct 2018;177:809–35. https://doi.org/10.1016/j.engstruct.2018.08.071.

[30] Aşıkoğlu A, Avşar Ö, Lourenço PB, Silva LC. Effectiveness of seismic retrofitting of a historical masonry structure: Kütahya Kurşunlu Mosque, Turkey. Bull Earthq Eng 2019;17:3365–95. https://doi.org/10.1007/S10518-019-00603-6/FIGURES/32.

[31] Haddad J, Cattari S, Lagomarsino S. Sensitivity and Preliminary Analyses for the Seismic Assessment of Ardinghelli Palace. RILEM Bookseries 2019;18:2412–21. https://doi.org/10.1007/978-3-319-99441-3_259/TABLES/3.

[32] Kita A, Cavalagli N, Venanzi I, Ubertini F. A new method for earthquake-induced damage identification in historic masonry towers combining OMA and IDA. Bull Earthq Eng 2021;19:5307–37. https://doi.org/10.1007/S10518-021-01167-0/FIGURES/16.

[33] Ponte M, Bento R, Vaz SD. A Multi-Disciplinary Approach to the Seismic Assessment of the National Palace of Sintra, International Journal of. Archit Herit 2021;15:757–78. https://doi.org/10.1080/15583058.2019.1648587.

[34] Ozcelik O, Misir IS, Yucel U, Durmazgezer E, Yucel G, Amaddeo C. Model updating of Masonry courtyard walls of the historical Isabey mosque using ambient vibration measurements. J Civ Struct Heal Monit 2022;2022:1–16. https://doi.org/10.1007/S13349-022-00610-3.

[35] Bartoli G, Betti M, Biagini P, Borghini A, Ciavattone A, Girardi M, et al. Epistemic Uncertainties in Structural Modeling: A Blind Benchmark for Seismic Assessment of Slender Masonry Towers. J Perform Constr Facil 2017;31. https://doi.org/10.1061/(ASCE)CF.1943-5509.0001049.

[36] Endo Y, Pelà L, Roca P. Review of Different Pushover Analysis Methods Applied to Masonry Buildings and Comparison with Nonlinear Dynamic Analysis. J Earthq Eng 2016;21:1234–55. https://doi.org/10.1080/13632469.2016.1210055.

[37] Lagomarsino S, Cattari S. Seismic Performance of Historical Masonry Structures Through Pushover and Nonlinear Dynamic Analyses, in: Perspectives on European Earthquake Engineering and Seismology. Vol. 39, 2015: pp. 265–292. https://doi.org/10.1007/978-3-319-16964-4_11.

[38] Maraş MM, Özmen A, Sayın E, Ayaz Y. Seismic Assessment of the Historical Sütlü Minaret Mosque. Periodica Polytechnica Civil Engineering 2022. https://doi.org/10.3311/PPci.19400.

[39] Grillanda N, Valente M, Milani G, Chiozzi A, Tralli A. Advanced numerical strategies for seismic assessment of historical masonry aggregates. Eng Struct 2020;212:110441. https://doi.org/10.1016/j.engstruct.2020.110441.

[40] Herrero Romero S. Teoría y práctica de la restauración de la Mezquita-Catedral de Córdoba durante el siglo XX. Universidad Politécnica de Madrid 2015. https://doi.org/10.20868/UPM.thesis.39987.

[41] Almagro Gorbea A, Arquitectura Al-Andalus, in: Catálogo Digital de Arquitectura RABASF, 2022.

[42] Kumavat HR, Chandak NR, Patil IT. Factors influencing the performance of rebound hammer used for non-destructive testing of concrete members: A review. Case Stud Constr Mater 2021;14:e00491.

[43] PROETISA, (n.d.). https://www.proetisa.com/proetisa-productos.php?ID=159 (accessed November 7, 2022).

[44] ARTeMIS Modal - Structural Vibration Solutions, (n.d.). https://svibs.com/ (accessed November 10, 2022).

[45] Sadeqi A, Esfandiari A, Sanayei M, Rashvand M. Automated operational modal analysis based on long-term records: A case study of Milad Tower structural health monitoring. Struct Control Health Monit 2022;29. https://doi.org/10.1002/STC.3037.

[46] Binda L, Cardani G, Proposta di una metodologia per la valutazione della qualità muraria. In: Reluis, progetto esecutivo 2005–2008, Linee guida per la compilazione della scheda di valutazione della qualita' muraria, Decembre, 2007.

[47] Swiss Society of Engineers and Architects (SIA), SIA 266/2; SN 505266/2 (in German), Zürich, Switzerland , 2012. http://shop.sia.ch/normenwerk/ingenieur/266-2_2012_d/D/Product (accessed November 30, 2022).

[48] Kržan M, Gostič S, Cattari S, Bosiljkov V. Acquiring reference parameters of masonry for the structural performance analysis of historical buildings. Bull Earthq Eng 2015;13:203–36. https://doi.org/10.1007/s10518-014-9686-x.

[49] European Union, Eurocode-6: Design of masonry structures. Part 1-1: General rules for reinforced and unreinforced masonry structures, Brussels, 2005.

[50] Lourenço PB, van Hees R, Fernandes F, Lubelli B. Characterization and Damage of Brick Masonry. In: Structural Rehabilitation of Old Buildings, Springer, 2014: pp. 109–130. https://doi.org/10.1007/978-3-642-39686-1_4.

[51] Kržan M, Gostič S, Bosiljkov V. Application of different in-situ testing techniques and vulnerability assessment of Kolizej palace in Ljubljana. Bull Earthq Eng 2015;13:389–410. https://doi.org/10.1007/s10518-014-9639-4.

[52] Jäger W, Marzahn G, Mauerwerk Bemessung nach DIN 1053-100 (in German), 2010.

[53] Schubert P. Eigenschaftswerte von Mauerwerk. Mauersteinen, Mauermörtel und Putzen, Mauerwerk-Kalender 2009;2009:1–27. https://doi.org/10.1002/9783433600306.CH1.

[54] Luque A, Cultrone G, Mosch S, Siegesmund S, Sebastian E, Leiss B. Anisotropic behaviour of White Macael marble used in the Alhambra of Granada (Spain): The

role of thermohydric expansion in stone durability. Eng Geol 2010;115:209–16. https://doi.org/10.1016/J.ENGGEO.2009.06.015.
[55] Huang C, Gong M, Chui Y, Chan F. Mechanical behaviour of wood compressed in radial direction-part I. New method of determining the yield stress of wood on the stress-strain curve. J Bioresources Bioproducts 2020;5:186–95. https://doi.org/10.1016/J.JOBAB.2020.07.004.
[56] Namari S, Drosky L, Pudlitz B, Haller P, Sotayo A, Bradley D, et al. Mechanical properties of compressed wood. Constr Build Mater 2021;301:124269. https://doi.org/10.1016/J.CONBUILDMAT.2021.124269.
[57] Fajfar P. A nonlinear analysis method for performance-based seismic design. Earthq Spectra 2000;16:573–92.
[58] European Union, Eurocode 8: Design of structures for earthquake resistance. Part 1: General rules, seismic actions and rules for buildings, Belgium, 2004.
[59] Spanish Ministry of Public Works [Ministerio de Fomento de España], Update of the seismic hazard maps [Actualización de mapas de peligrosidad sísmica de España], Spain, Spain, 2012.
[60] European Union, Eurocode-8: Design of structures for earthquake resistance. Part 3: Assessment and retrofitting of buildings, Brussels, Belgium, 2005. http://www.phd.eng.br/wp-content/uploads/2014/07/en.1998.3.2005.pdf.
[61] McKenna F, Fenves GL, Scott MH. OpenSees: Open system for earthquake engineering simulation. Pacific Earthquake Engineering Research Center, University of California, Berkeley, CA, 2000. https://opensees.berkeley.edu/ (accessed November 21, 2019).
[62] Rhino - Rhinoceros 3D, (n.d.). https://www.rhino3d.com/ (accessed November 10, 2022).
[63] Cattari S, Camilletti D, D'Altri AM, Lagomarsino S. On the use of continuum Finite Element and Equivalent Frame models for the seismic assessment of masonry walls. J Build Eng 2021;43:102519. https://doi.org/10.1016/j.jobe.2021.102519.
[64] Petracca M, Candeloro F, Camata G. "STKO user manual". ASDEA Software Technology, Pescara, Italy, 2017. https://asdeasoft.net/pdf/STKOUserManual.pdf (accessed July 8, 2020).
[65] Romero Sánchez E, Morales Esteban A, Navarro Casas J. Analysis of the Historical Settlements of the Giralda. Int J Archit Herit 2022:1–19. https://doi.org/10.1080/15583058.2022.2034070.
[66] Lourenco PB. Computational strategies for masonry structures, TU Delf, 1996. https://repository.tudelft.nl/islandora/object/uuid%3A4f5a2c6c-d5b7-4043-9d06-8c0b7b9f1f6f (accessed March 24, 2023).
[67] Romero Sanchez E, Bento R, Morales Esteban A, Navarro Casas J. Numerical modelling for the seismic assessment of complex masonry heritage buildings: the case study of the Giralda tower. Bull Earthq Eng 2023. Under review.
[68] Petracca M, Pelà L, Rossi R, Zaghi S, Camata G, Spacone E. Micro-scale continuous and discrete numerical models for nonlinear analysis of masonry shear walls. Constr Build Mater 2017;149:296–314. https://doi.org/10.1016/j.conbuildmat.2017.05.130.
[69] Bartoli G, Betti M, Vignoli A. A numerical study on seismic risk assessment of historic masonry towers: a case study in San Gimignano. Bull Earthq Eng 2016;14:1475–518. https://doi.org/10.1007/s10518-016-9892-9.
[70] Petracca M, Pelà L, Rossi R, Oller S, Camata G, Spacone E. Multiscale computational first order homogenization of thick shells for the analysis of out-of-plane loaded masonry walls. Comput Methods Appl Mech Eng 2017;315:273–301. https://doi.org/10.1016/j.cma.2016.10.046.
[71] Standoli G, Salachoris GP, Masciotta MG, Clementi F. Modal-based FE model updating via genetic algorithms: Exploiting artificial intelligence to build realistic numerical models of historical structures. Constr Build Mater 2021;303:124393. https://doi.org/10.1016/J.CONBUILDMAT.2021.124393.
[72] Salachoris GP, Standoli G, Betti M, Milani G, Clementi F. Evolutionary numerical model for cultural heritage structures via genetic algorithms: a case study in central Italy. Bull Earthq Eng 2023. https://doi.org/10.1007/s10518-023-01615-z.
[73] Ferrante A, Loverdos D, Clementi F, Milani G, Formisano A, Lenci S, et al. Discontinuous approaches for nonlinear dynamic analyses of an ancient masonry tower. Eng Struct 2021;230:111626. https://doi.org/10.1016/j.engstruct.2020.111626.
[74] Ferrante A, Schiavoni M, Bianconi F, Milani G, Clementi F. Influence of Stereotomy on Discrete Approaches Applied to an Ancient Church in Muccia, Italy. J Eng Mech 2021;147. https://doi.org/10.1061/(ASCE)EM.1943-7889.0002000.
[75] Requena-Garcia-Cruz MV, Romero-Sánchez E, Morales-Esteban A. Numerical investigation of the contribution of the soil-structure interaction effects to the seismic performance and the losses of RC buildings. Dev Built Environ 2022;12:100096. https://doi.org/10.1016/j.dibe.2022.100096.
[76] Requena-Garcia-Cruz MV, Bento R, Durand-Neyra P, Morales-Esteban A. Analysis of the soil structure-interaction effects on the seismic vulnerability of mid-rise RC buildings in Lisbon. Structures 2022;38:599–617. https://doi.org/10.1016/j.istruc.2022.02.024.